2021 2nd Season Stock Assessment

Falkland calamari

(*Doryteuthis gahi*)

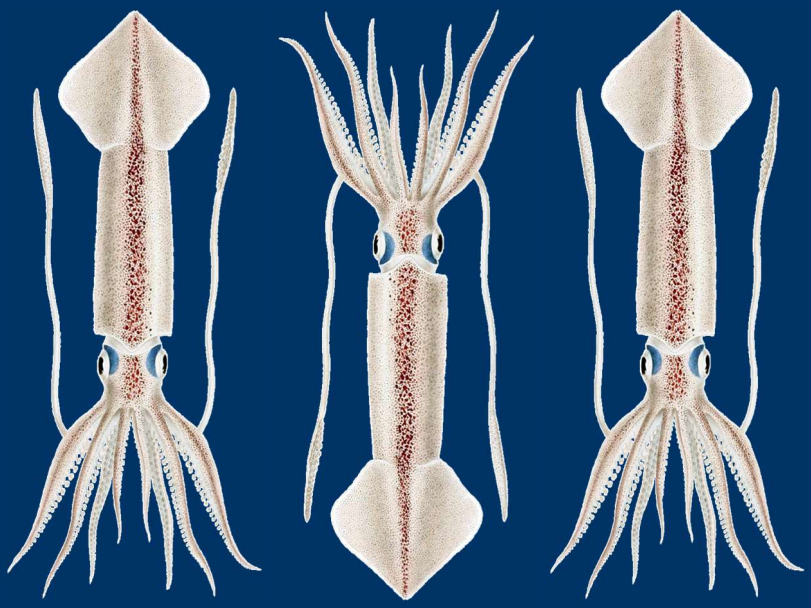

S2 - 2021 - LOL

Andreas Winter

Natural Resources - Fisheries
Falkland Islands Government
Stanley, Falkland Islands

November 2021

Index

Summary

1) The 2021 second season *Doryteuthis gahi* fishery (X license) was open from July 28th and closed by directed order on September 29th. Compensatory flex days for mechanical breakdown, bad weather, and vaccinations resulted in 22 vessel-days taken after September 29th, with the last two vessels fishing as late as October 3rd.
2) 34,665.5 tonnes of *D. gahi* catch were reported in the 2021 X-license fishery, plus 84.3 t in a brief in-season E-license fishery, giving an average CPUE of 35.4 t vessel-day^{-1}. Total catch was the fourth-highest for a 2nd season since 2004, and average CPUE was the third-highest for a 2nd season since 2004. 86.1% of *D. gahi* catch and 77.1% of fishing effort were taken south of 52º S; 13.9% of *D. gahi* catch and 22.9% of fishing effort were taken north of 52º S. Four days in the north, by the entire fleet, were ordered as a test fishery.
3) In the south sub-area, four depletion periods / immigrations were inferred on July 28th (start of the season), August 4th, August 20th and September 13th. In the north sub-area, two depletion periods / immigrations were inferred on July 28th and August 20th.
4) Approximately 31,535 tonnes of *D. gahi* (95% confidence interval: 21,781 to 45,516 t) were estimated to have immigrated into the Loligo Box after the start of 2nd season 2021, of which 26,283 t in the south sub-area and 5,252 t in the north sub-area.
5) The escapement biomass estimate for *D. gahi* remaining in the Loligo Box at the end of 2nd season 2021 was: Maximum likelihood of 38,449 tonnes, with a 95% confidence interval of 31,946 to 64,309 tonnes.
   The risk of *D. gahi* escapement biomass at the end of the season being less than 10,000 tonnes was estimated at effectively zero.

Introduction

Second season (X licence) of the 2021 *Doryteuthis gahi* fishery (Patagonian longfin squid – colloquially *Loligo*) opened on July 28th, with 16 vessels entering the fishery. One regular vessel was replaced for the first eight days by an alternate vessel while proceeding with health protocols on-board. Throughout the season, flex days were requested for mechanical breakdowns, bad weather (eleven on August 8th; Figure 1), and for the first time; crew vaccinations. A total of 22 fishing days were taken after scheduled closure on September 29th with the last two vessels fishing on October 3rd. The last few days also included a brief experimental fishery by one vessel, *New Polar*, to test net improvements for seabird mitigation (Iriarte and Shcherbich, FIFD, in preparation).

All X-license vessels were required to embark a Marine Mammal Observer to monitor presence and incidental capture of pinnipeds, and additionally, SEDs were mandatory for the duration of the season. Ultimately, 43[a] pinniped mortalities were reported for the season: 41 South American fur seals *Arctocephalus australis*, and 2 Southern sea lions *Otaria flavescens*.

Total reported *D. gahi* catch under second season X licence, plus the brief experimental fishery, was 29,925 south + 4,825 north = 34,750 tonnes (Table 1), corresponding to an average CPUE of 34750 / 982 = 35.4 tonnes vessel-day^{-1}. Total catch was the highest for a 2nd season since 2018, and average CPUE was the highest for a 2nd season since 2019.

Figure 1 [below]. Fish Ops chart display (right) and wind speed vector plots (Copernicus Marine Service) (left) on August 8th, when only five vessels fished.

[a] The total includes indirect mortalities as some females were killed in lactating condition and/or pregnant, and their pups are therefore presumed to not survive either (V. Iriarte, FIFD, pers. comm.).

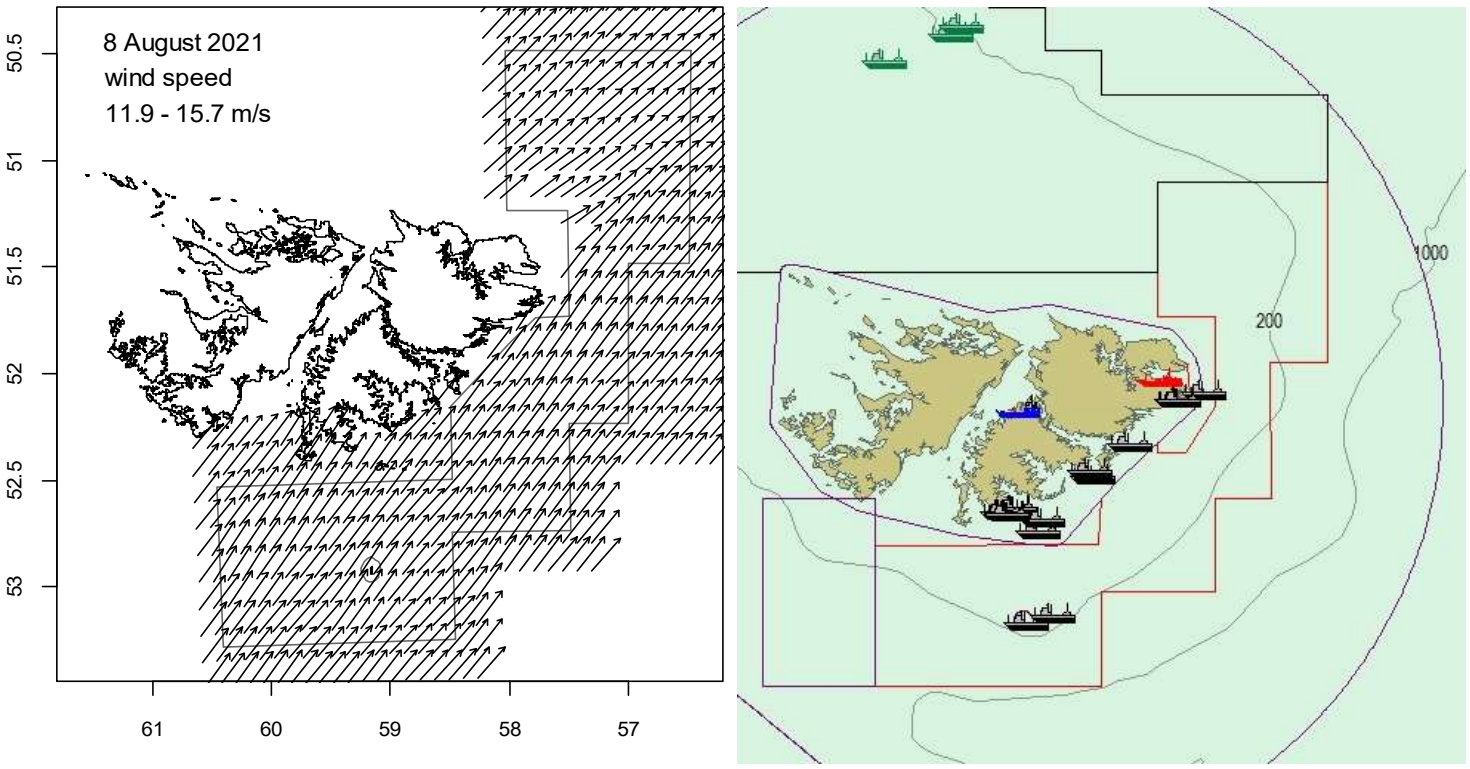

Table 1. *D. gahi* season comparisons since 2004, when fisheries management was assumed by the FIFD. Days: total number of calendar days open to licensed *D. gahi* fishing including (since 1st season 2013) optional flex days; V-Days: aggregate number of licensed *D. gahi* fishing days reported by all vessels for the season. Entries in italics are seasons closed by emergency order.

	Season 1			Season 2		
	Catch (t)	Days	V-Days	Catch (t)	Days	V-Days
2004	7,152	46	625	17,559	78	1271
2005	24,605	45	576	29,659	78	1210
2006	19,056	50	704	*23,238*	*53*	*883*
2007	17,229	50	680	*24,171*	*63*	*1063*
2008	24,752	51	780	26,996	78	1189
2009	12,764	50	773	*17,836*	*59*	*923*
2010	28,754	50	765	36,993	78	1169
2011	15,271	50	771	*18,725*	*70*	*1099*
2012	34,767	51	770	35,026	78	1095
2013	19,908	53	782	19,614	78	1195
2014	28,119	59	872	19,630	71	1099
2015	*19,383*	*57*	*871**	*10,190*	*42*	*665*
2016	22,616	68	1020	23,089	68	1004
2017	39,433	68	999†	24,101	69	1002‡
2018	43,085	69	975	35,828	68	977
2019	55,586	68	953	*24,748*	*43*	*635*
2020	29,116	68	1012	29,759	69	993
2021	*59,587*	*62*	*891*	34,750	68	982⁋

* Does not include C-license catch or effort after the target was switched from *D. gahi* to *Illex*.
† Includes two vessel-days of experimental fishing for juvenile toothfish.
‡ Includes one vessel-day of experimental fishing for juvenile toothfish.
⁋ Includes three vessel-days of experimental fishing for SED improvement.

Assessment of the Falkland Islands *D. gahi* stock was conducted with depletion time-series models as in previous seasons (Agnew et al. 1998, Roa-Ureta and Arkhipkin 2007; Arkhipkin et al. 2008), and in other squid fisheries (cited in Arkhipkin et al. 2021). Because *D. gahi* has an annual life cycle (Patterson 1988, Arkhipkin 1993), stock cannot be derived from a standing biomass carried over from prior years (Rosenberg et al. 1990, Pierce and Guerra 1994). The depletion model instead calculates an estimate of population abundance over time by evaluating what levels of abundance and catchability must be present to sustain the observed rate of catch. Depletion modelling of the *D. gahi* target fishery is used both in-season and for the post-season summary, with the objective of maintaining an escapement biomass of 10,000 tonnes *D. gahi* at the end of each season as a conservation threshold (Agnew et al. 2002, Barton 2002).

Methods

The depletion model formulated for the Falklands *D. gahi* stock is based on the equivalence:

$$C_{day} = q \times E_{day} \times N_{day} \times e^{-M/2} \quad \textbf{(1)}$$

where q is the catchability coefficient, M is the natural mortality rate (considered constant at 0.0133 day^{-1}; Roa-Ureta and Arkhipkin 2007), and C_{day}, E_{day}, N_{day} are respectively catch (numbers of squid), fishing effort (numbers of vessels), and abundance (numbers of squid) per day. The catchability coefficient q summarized the range of variation of all trawls taken by the fishing fleet in this season.

In its basic form (DeLury 1947) the depletion model assumes a closed population in a fixed area for the duration of the assessment. However, the assumption of a closed population is imperfectly met in the Falkland Islands fishery, where stock analyses have often shown that *D. gahi* groups arrive in successive waves after the start of the season (Roa-Ureta 2012; Winter and Arkhipkin 2015). Arrivals of successive groups are inferred from discontinuities in the catch data. Fishing on a single, closed cohort would be expected to yield gradually decreasing CPUE, but gradually increasing average individual sizes, as the squid grow. When instead these data change suddenly, or in contrast to expectation, the immigration of a new group to the population is indicated (Winter and Arkhipkin 2015).

In the event of a new group arrival, the depletion calculation must be modified to account for this influx. Modification is done using a simultaneous algorithm that adds new arrivals on top of the stock previously present, and posits a common catchability coefficient for the entire depletion time-series. If two depletions are included in the same model (i.e., the stock present from the start plus a new group arrival), then:

$$C_{day} = q \times E_{day} \times (N1_{day} + (N2_{day} \times i2|_0^1)) \times e^{-M/2} \quad \textbf{(2)}$$

where i2 is a dummy variable taking the values 0 or 1 if 'day' is before or after the start day of the second depletion. For more than two depletions, $N3_{day}$, i3, $N4_{day}$, i4, etc., would be included following the same pattern.

The season depletion likelihood function was calculated as the difference between actual catch numbers reported and catch numbers predicted from the model (Equation **2**), statistically corrected by a factor relating to the number of days of the depletion period (Roa-Ureta 2012):

$$\text{minimization} \rightarrow \ ((n\text{Days} - 2)/2) \times \log\left(\sum_{days}\left(\log(\text{predicted } C_{day}) - \log(\text{actual } C_{day})\right)^2\right) \quad \textbf{(3)}$$

The stock assessment was set in a Bayesian framework (Punt and Hilborn 1997), whereby results of the season depletion model are conditioned by prior information on the stock; in this case the information from the pre-season survey.

The likelihood function of prior information was calculated as the normal distribution of the difference between catchability derived from the survey abundance estimate ($_{\text{prior}}\,q$), and catchability derived from the season depletion model ($_{\text{depletion}}\,q$). Applying this difference requires both the survey and the season to be fishing the same stock with the same gear. Catchability, rather than abundance N, is used for calculating prior likelihood because catchability informs the entire season time series; whereas N from the survey only informs the first in-season depletion period – subsequent immigrations and depletions are independent of the abundance that was present during the survey. Thus, the prior likelihood function was:

$$\text{minimization} \rightarrow \ \frac{1}{\sqrt{2\pi \cdot SD_{\text{prior q}}{}^2}} \times \exp\left(-\frac{\left(_{\text{depletion}}\,q - {}_{\text{prior}}\,q\right)^2}{2 \cdot SD_{\text{prior q}}{}^2}\right) \quad \textbf{(4)}$$

where the standard deviation of catchability prior ($SD_{\text{prior q}}$) was calculated from the Euclidean sum (Carlson 2014) of the survey prior estimate uncertainty, the variability in catches on the season start date, and the uncertainty in the natural mortality M estimate over the number of days mortality discounting (Appendix Equation **A5**).

Bayesian optimization of the depletion was calculated by jointly minimizing Equations **3** and **4**, using the Nelder-Mead algorithm in R programming package 'optimx' (Nash and Varadhan 2011). Relative weights in the joint optimization were assigned to Equations **3** and **4** as the converse of their coefficients of variation (CV), i.e., the CV of the prior became the weight of the depletion model and the CV of the depletion model became the weight of the prior. Calculations of the depletion CVs are described in Equations **A8-S** and **A8-N**. Because a complex model with multiple depletions may converge on a local minimum rather than global minimum, the optimization was stabilized by running a feed-back loop that set the q and N parameter outputs of the Bayesian joint optimization back into the in-season-only minimization (Equation **3**), re-calculated the in-season-only minimization, then re-calculated the Bayesian joint optimization, and continued this process until both the in-season minimization and the joint optimization remained unchanged.

With actual C_{day}, E_{day} and M being fixed parameters, the optimization of Equation **2** using Equations **3** and **4** produces estimates of q and N1, N2, …, etc. Numbers of squid on the final day (or any other day) of a time series are then calculated as the numbers N of the depletion start days discounted for natural mortality during the intervening period, and subtracting cumulative catch also discounted for natural mortality (CNMD). Taking for example a two-depletion period:

$$\begin{aligned} N_{\text{final day}} &= N1_{\text{start day 1}} \times e^{-M\,(\text{final day} - \text{start day 1})} \\ &\quad + N2_{\text{start day 2}} \times e^{-M\,(\text{final day} - \text{start day 2})} \\ &\quad - CNMD_{\text{final day}}, \end{aligned} \quad \textbf{(5)}$$

$$CNMD_{\text{day 1}} = 0$$

$$CNMD_{\text{day x}} = CNMD_{\text{day x-1}} \times e^{-M} + C_{\text{day x-1}} \times e^{-M/2} \quad \textbf{(6)}$$

$N_{\text{final day}}$ is then multiplied by the average individual weight of squid on the final day to give biomass. Daily average individual weight is obtained from length / weight conversion of mantle lengths measured in-season by observers, and also derived from in-season commercial data as the proportion of product weight that vessels reported per market size category[b]. Observer mantle lengths are scientifically more accurate, but restricted to a partial sample of trawls. Commercially proportioned mantle lengths are relatively less accurate, but cover every trawl of the entire fishing fleet every day. Therefore, both sources of data are used (see Appendix – *Doryteuthis gahi* individual weights).

Distributions of the likelihood estimates from joint optimization (i.e., measures of their statistical uncertainty) were computed using a Markov Chain Monte Carlo (MCMC) (Gamerman and Lopes 2006), a method that is commonly employed for fisheries assessments (Magnusson et al. 2013). MCMC is an iterative process which generates random stepwise changes to the proposed outcome of a model (in this case, the q and N of *D. gahi* squid) and at each step, accepts or nullifies the change with a probability equivalent to how well the change fits the model parameters compared to the previous step. The resulting sequence of accepted or nullified changes (i.e., the 'chain') approximates the likelihood distribution of the model outcome. The MCMC of the depletion models were run for 200,000 iterations; the first 1000 iterations were discarded as burn-in sections (initial phases over which the algorithm stabilizes); and the chains were thinned by a factor equivalent to the maximum of either 5 or the inverse of the acceptance rate (e.g., if the acceptance rate was 12.5%, then every eighth (0.125^{-1}) iteration was retained) to reduce serial correlation. For each model three chains were run; one chain initiated with the parameter values obtained from the joint optimization of Equations **3** and **4**, one chain initiated with these parameters ×2, and one chain initiated with these parameters ×¼. Convergence of the three chains was accepted if the variance among chains was less than 10% higher than the variance within chains (Brooks and Gelman 1998). When convergence was satisfied the three chains were combined as one final set. Equations **5**, **6**, and the multiplication by average individual weight were applied to the CNMD and to each iteration of N values in the final set, and the biomass outcomes from these calculations represent the distribution of the estimate.

Depletion models and likelihood distributions were calculated separately for north and south sub-areas of the Loligo Box fishing zone, as *D. gahi* sub-stocks emigrate from different spawning grounds and remain to an extent segregated (Arkhipkin and Middleton 2002). However, q_{prior} was calculated for the north and south sub-areas combined, rather than separately (Equation **A4**). As fishing tends to start predominantly in one or the other sub-area, rather than the fleet spreading itself evenly, separately computed north and south qs_{prior} were susceptible to arbitrary differences. Total escapement biomass was then defined as the aggregate biomass of *D. gahi* on the last day of the season for north and south sub-areas combined. North and south biomasses are not assumed to be uncorrelated however (Shaw et al. 2004), and therefore north and south likelihood distributions were added semi-randomly in proportion to the strength of their day-to-day correlation (see Winter 2014, for the semi-randomization algorithm).

Figure 2 [next page]. Spatial distribution of *D. gahi* 2021 2nd-season trawls, colour-scaled to catch weight (maximum = 65.5 tonnes). 2765 trawl catches were taken during the season. The 'Loligo Box' fishing zone and 52 ºS parallel delineating the boundary between north and south assessment sub-areas, are shown in grey.

[b] First reported for Falkland Islands *D. gahi* by Payá (2006). Also used in some finfish commercial fisheries, see Plet-Hansen et al. 2018.

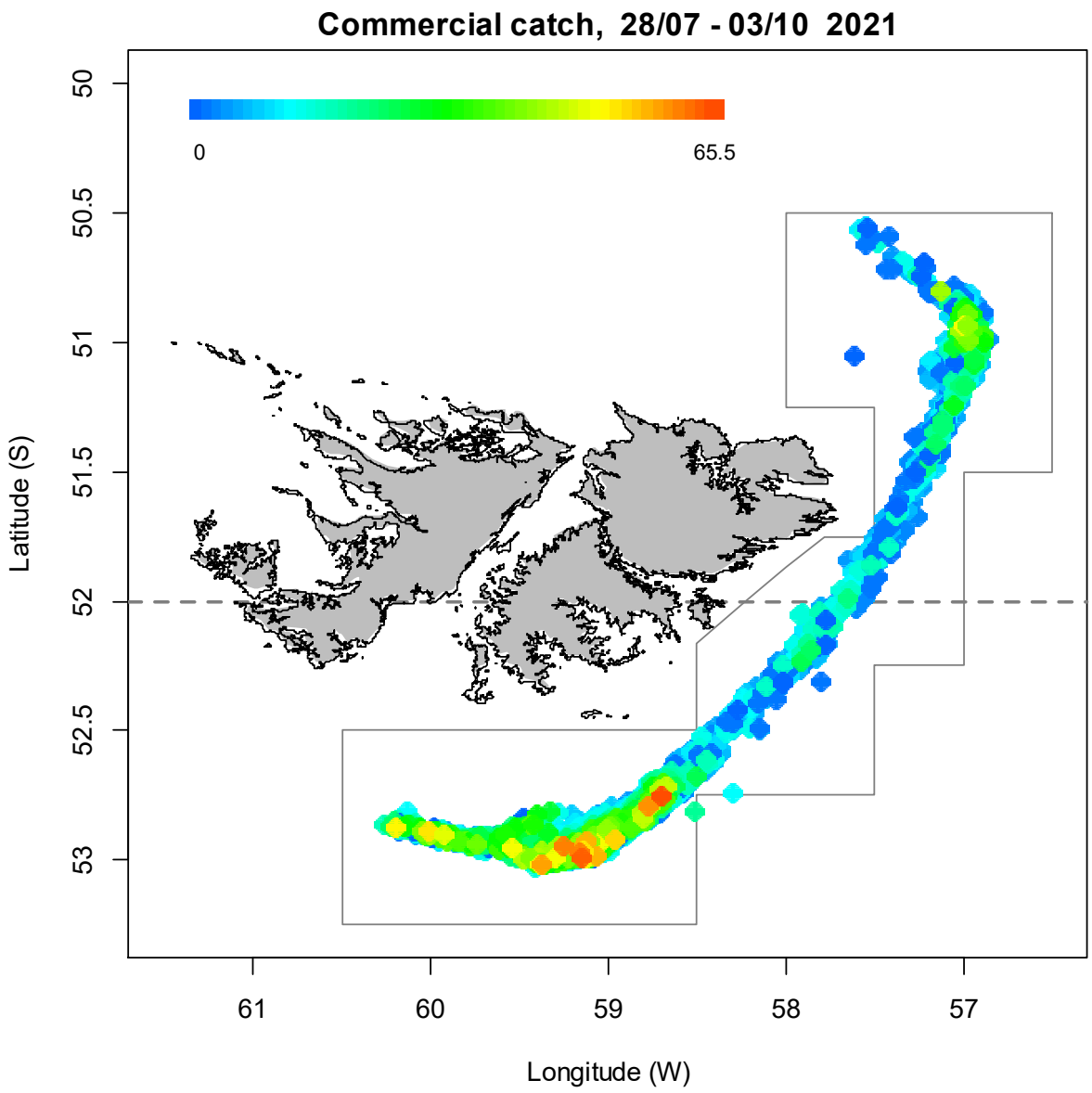

Stock assessment

Catch and effort

The north sub-area was fished on 40 of 68 season-days, for 13.9% of total catch (4824.7 t *D. gahi*) and 22.9% of effort (224.8 vessel-days) (Figures 2 and 3). The south sub-area was fished on 63 of the 68 season-days, for 86.1% of total catch (29925.1 t *D. gahi*) and 77.1% of effort (757.2 vessel-days). During four consecutive days of 2nd season 2021 (September 9th to 12th), the fleet was ordered to move from south to north and 'test' fish the north given its otherwise low level of effort (Figure 3). Fishing companies were given the option of selecting eight vessels to move north for those four days, but chose to send all sixteen (A. Arkhipkin, FIFD, pers. comm.).

The high preponderance of season catch and effort south is comparable to 2nd season 2019 (Winter 2019), but differs with respect to its strong contrast from the pre-season survey. The 2nd pre-season 2021 survey showed an exceptionally high proportion of biomass estimated north (67.1%; Winter et al. 2021), whereas the 2nd pre-season 2019 survey more typically had the highest proportion of biomass south (Goyot et al. 2019), as did the subsequent season.

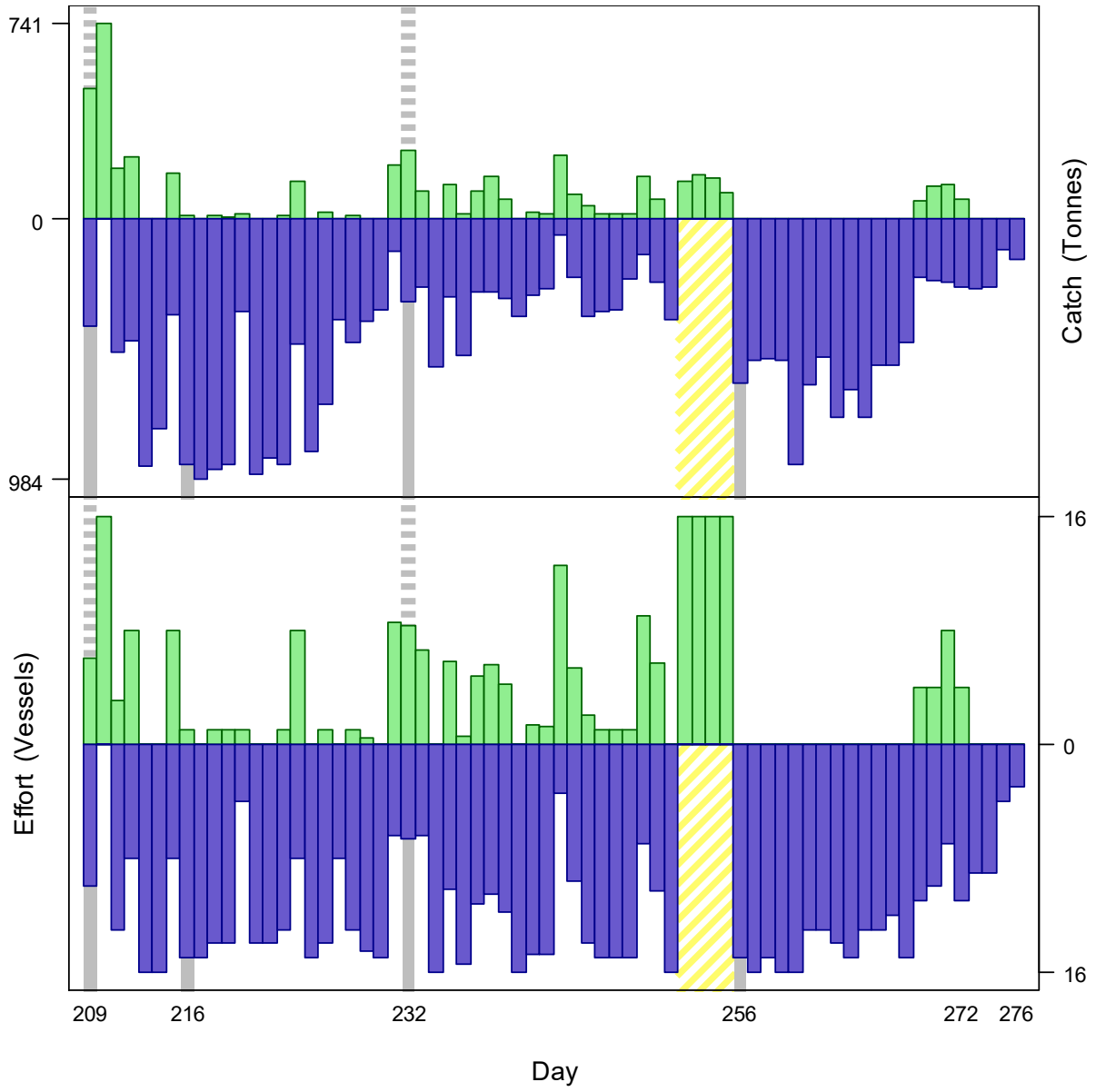

Figure 3. Daily total *D. gahi* catch and effort distribution by assessment sub-area north (green) and south (purple) of the 52° S parallel during 2nd season 2021. The season was open from July 28th (chronological day 209) with directed closure scheduled on September 29th (day 272), with flex days until October 3rd (day 276). Yellow shading: temporary exclusion of the south sub-area. As many as 16 vessels fished per day north; as many as 16 vessels fished per day south. As much as 741 tonnes *D. gahi* was caught per day north; as much as 984 tonnes *D. gahi* was caught per day south.

A contrast between pre-season and in-season distribution was also present last year (Winter et al. 2020, Winter 2020), although much more attenuated. Notably, 2nd seasons of 2020 and 2021 have been the only two calamari seasons reporting >200 t hake (*Merluccius hubbsi*) catch (Winter 2020; Table A1 below). In both of these 2nd seasons, hake, as proportions of total catches, were significantly correlated with latitude northwards as well as depth (Figure 4, Table 2). In 2nd season 2021, but not 2020, rock cod (*Patagonotothen ramsayi*) was significantly correlated with latitude southwards as well as depth (Figure 4, Table 2). Rock cod catch was about 3× higher in 2nd season 2021 than 2020 (whereby both were relatively low compared to earlier years). The results suggest that northern concentrations of *D. gahi* were

reduced by hake, or the hake presence made calamari fishing uneconomical, especially in deeper water, and the effect may be increased by an opposite latitudinal trend of rock cod.

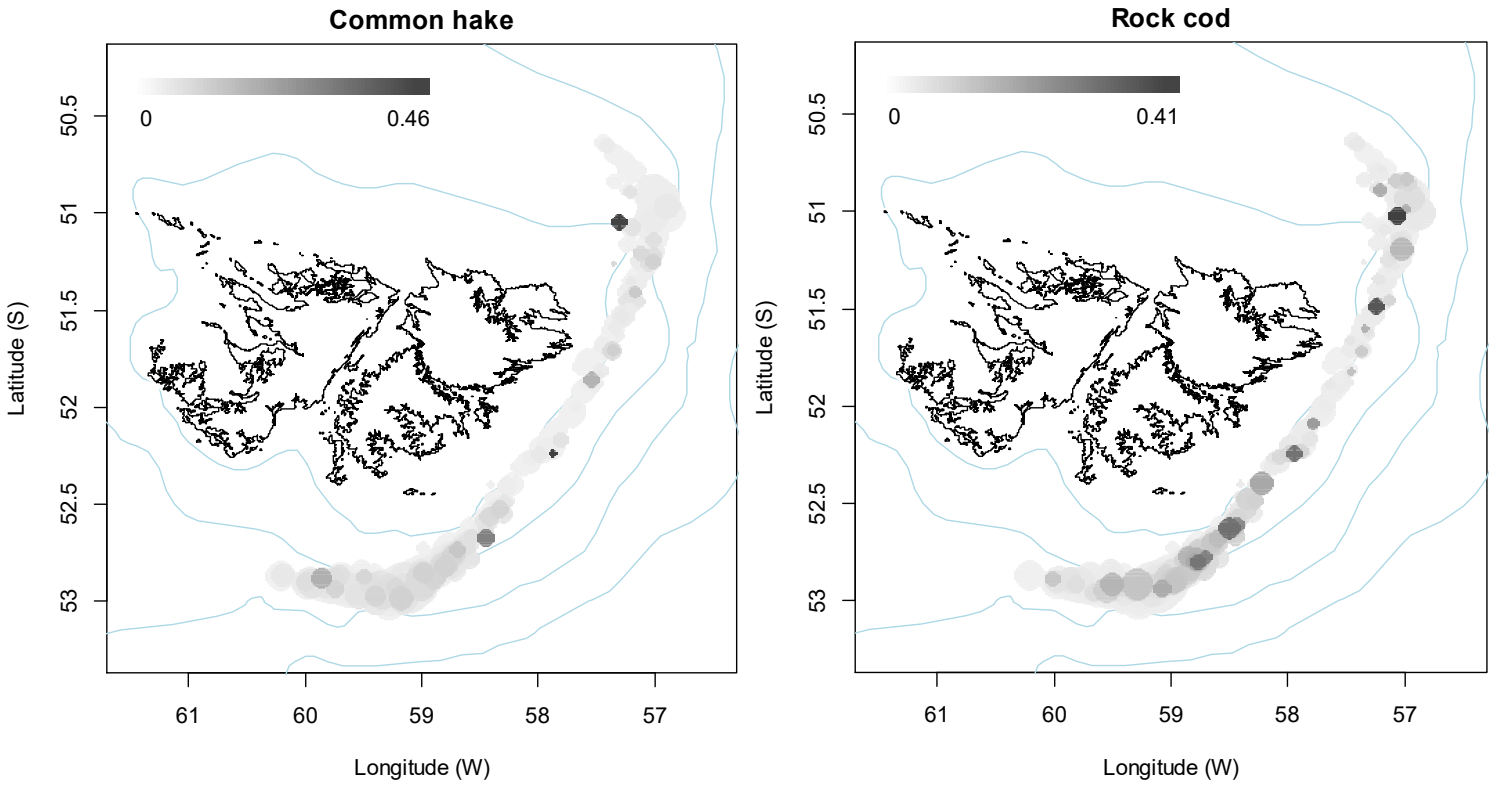

Figure 4. Proportions of common hake (left) and rock cod (right) in total catches per daily catch report (N = 982; cf. V-Days in Table 1). Locations are averages of trawl positions each report day, and square-root proportional size to total catches. Blue lines: bathymetry 100 m, 200 m, 500 m, and 1000 m.

Table 2. Generalized linear models of predictor variables cumulative day, latitude, longitude, and depth on the catches of hake and rock cod as proportions of total catches, per vessel report day in 2nd seasons 2020 and 2021.

Year	Predictor	Hake			Rock cod		
		Estimate	|t|	p (> |t|)	Estimate	|t|	p (> |t|)
2020	Cum. day	–0.60e-4	1.83	> 0.050	+1.54e-4	6.30	< 0.001
	Lat	+1.49e-2	6.88	< 0.001	+1.24e-4	0.08	> 0.500
	Lon	–1.13e-2	5.73	< 0.001	+2.43e-3	1.65	> 0.100
	Depth	+4.01e-4	19.03	< 0.001	+1.49e-4	9.43	< 0.001
2021	Cum. day	–3.29e-5	0.70	> 0.400	+4.78e-4	8.03	< 0.001
	Lat	+9.31e-3	2.37	< 0.020	–2.54e-2	5.08	< 0.001
	Lon	+7.30e-4	0.24	> 0.500	+2.98e-2	7.75	< 0.001
	Depth	+4.30e-4	9.97	< 0.001	+4.09e-4	7.44	< 0.001

Data

982 vessel-days were fished during the season (Table 1), with a median of 16 vessels per day (mean 14.95). Vessels reported daily catch totals to the FIFD and electronic logbook data that

included trawl times, positions, depths, and product weight by market size categories. Four FIG observers were deployed on four vessels in the fishing season for a total of 60 sampling days[c] (Evans 2021, Claes 2021, Matošević 2021, Santana in prep.). Throughout the 68 days of the season, 15 days had no FIG observer sampling, 46 days had 1 FIG observer sampling, and 7 days had two FIG observers sampling. Except for seabird days FIG scientific observers were tasked with sampling 200 *D. gahi* at two stations daily (400 specimens per day); reporting their maturity stages, sex, and lengths to 0.5 cm. Contract marine mammal observers were tasked with measuring 200 unsexed lengths of *D. gahi* per day. The length-weight relationship for converting observer and commercially proportioned lengths was combined from 2nd pre-season and season length-weight data of both 2020 and 2021, as 2021 data became available progressively with on-going observer coverage. The final parameterization of the length-weight relationship included 6122 measures from 2020 and 4538 measures from 2021, giving:

$$\text{weight (kg)} = 0.18165 \times \text{length (cm)}^{2.17511} / 1000 \quad \textbf{(7)}$$

with a coefficient of determination $R^2 = 95.0\%$.

Group arrivals / depletion criteria

Start days of depletions - following arrivals of new *D. gahi* groups - were judged primarily by daily changes in CPUE, with additional information from sex proportions, maturity, and average individual squid sizes. CPUE was calculated as metric tonnes of *D. gahi* caught per vessel per day. Days were used rather than trawl hours as the basic unit of effort. Commercial vessels do not trawl standardized duration hours, but rather durations that best suit their daily processing requirements. An effort index of days is therefore more consistent (FIFD 2004, Winter and Arkhipkin 2015). Inclusion of additional depletion starts was evaluated by improvement of the Akaike information criterion (Akaike 1973) on model fit. However, when the model is used for in-season monitoring, a new depletion start will almost certainly give a poorer AIC until a number of days have passed for better fit to supersede the penalty of the additional parameter. Improvement was therefore defined as showing a trend towards relatively lower AIC over progressive days rather than necessarily an outright lower AIC, so that depletion starts could be included as soon as their relevance was evident, and align the in-season model as soon as possible with the final post-season model.

Four days in the south and two days in the north were ultimately identified that represented the onset of significant immigrations / depletions throughout the season. Two other days in the south and one in the north were evaluated, but did not meet the AIC criterion. The very last day of fishing in the south had a high CPUE peak, but this was considered a tactical catch and not considered as a further immigration event.

- The first depletion start south was set on day 209 (July 28th), the first day of the season with ten vessels fishing south. CPUE was average (Figure 5); individual weights and maturities were near their minima for the season (Figure 6A, 6B, 6D).
- The second depletion start south was identified on day 216 (August 4th). CPUE increased sharply from the day before to its highest of the season to that date (Figure 5). Average individual observer weight showed a sudden and temporary increase from the day before (Figure 6B) whereas average commercial weight had undergone a

[c] Not counting seabird days (every fourth day).

sudden dip the day before (Figure 6A). The proportion of females decreased sharply on day 216 (Figure 6C).

- The third depletion start south was identified on day 232 (August 20th). CPUE increased sharply from the day before following steady declines over more than a week (Figure 5). Average individual observer-measured weights, proportion of females, and maturity all showed pronounced increases from the day before (Figure 6B, 6C, 6D).
- The fourth depletion start south was identified after resumption of fishing in the south on day 256 (September 13th), and set by default to that date. CPUE was the highest in more than three weeks (Figure 5). Average individual commercial weights and maturities were distinctly lower than before the four-day break (Figure 6A, 6D).

- The first depletion start north was set on day 209 (July 28th), the first day of the season with six vessels fishing north. CPUE was the highest in the north of the entire season (Figure 5).
- The second depletion start north was identified on day 232 (August 20th), concurrently with a depletion start in the south, showing an increase in CPUE (Figure 5). The day before, female individual average weight, female proportion, and female average maturity had all been the lowest of the season (Figure 6B, 6C, 6D).

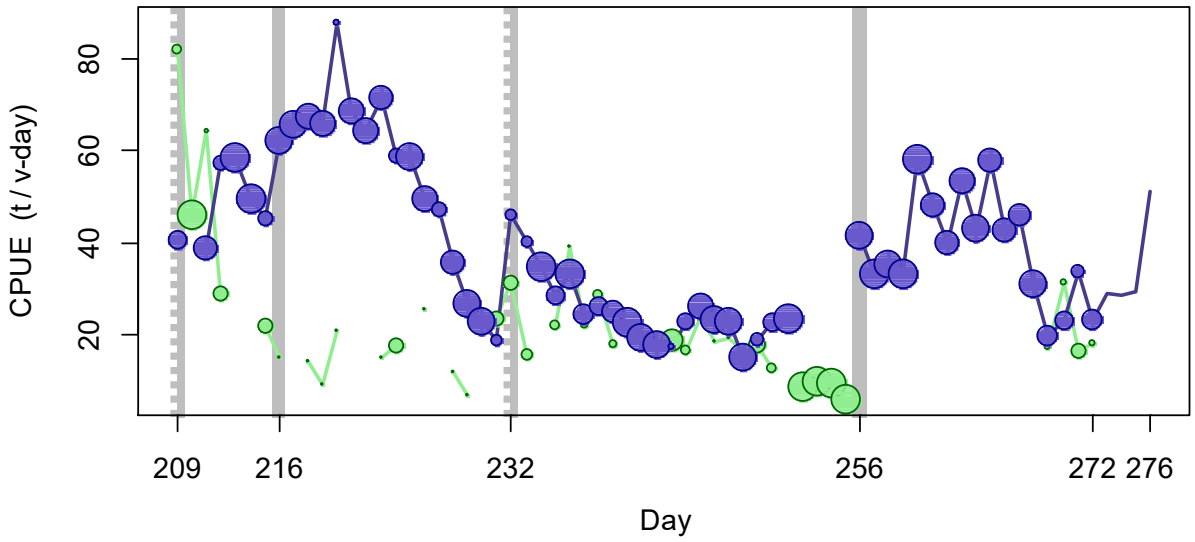

Figure 5. CPUE in metric tonnes per vessel per day, by assessment sub-area north (green) and south (purple) of 52º S latitude. Circle sizes are proportioned to numbers of vessels fishing. Data from consecutive days are joined by line segments. Broken grey bars indicate the starts of in-season depletions north. Solid grey bars indicate the starts of in-season depletions south.

Figure 6 [next page]. A: Average individual *D. gahi* weights (kg) per day from commercial size categories. B: Average individual *D. gahi* weights (kg) by sex per day from FIG observer sampling. C: Proportions of female *D. gahi* per day from FIG observer sampling. D: Average maturity index value (Lipiński 1979) by sex per day from FIG observer sampling. Males: triangles, females: squares, combined: circles. Thick lines (B) are unsexed measurements from contract marine mammal observer sampling. North sub-area: green, south sub-area: purple. Data from consecutive days are joined by line segments. Broken grey bars: the starts of in-season depletions north. Solid grey bars: the starts of in-season depletions south.

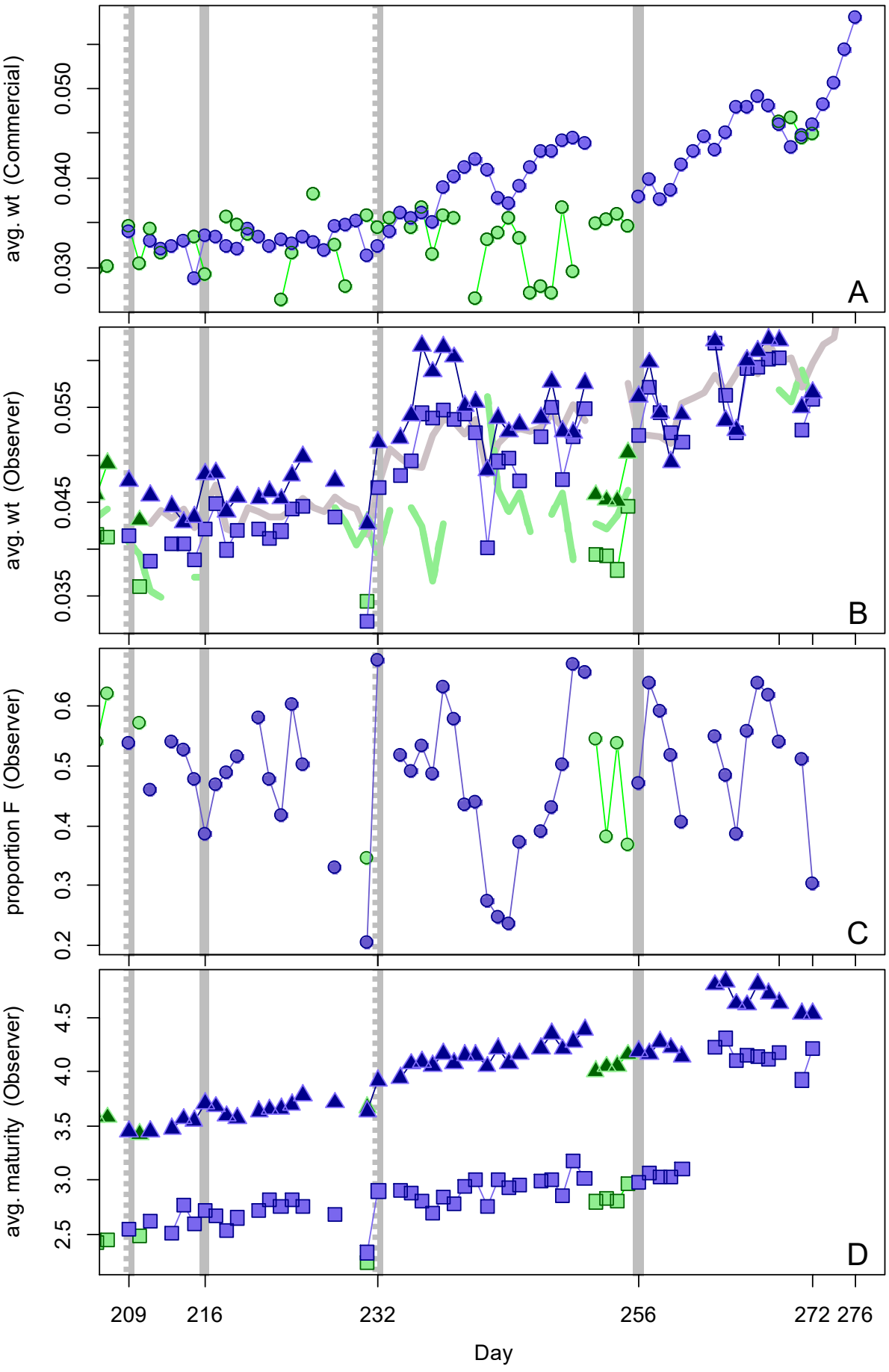
avg. wt (Commercial)
0.030
0.040
0.050
A
avg. wt (Observer)
0.035
0.045
0.055
B
proportion F (Observer)
0.2
0.3
0.4
0.5
0.6
C
avg. maturity (Observer)
2.5
3.0
3.5
4.0
4.5
D
209
216
232
256
272
276
Day

Depletion analyses
South

In the south sub-area, the maximum likelihood posterior ($_{Bayesian}$ q $_S$ = 1.523 × 10^{-3}; Figure 7-left, and Equation **A9-S**) was intermediate between the pre-season prior ($_{prior}$ q = 0.734 × 10^{-3}; Figure 7-left, and Equation **A4**) and the in-season depletion ($_{depletion}$ q $_S$ = 2.479 × 10^{-3}; Figure 7-left, and **A6-S**); even though the prior weight in the model was 4× lower than the in-season weight (Equations **A5** and **A8-S**).

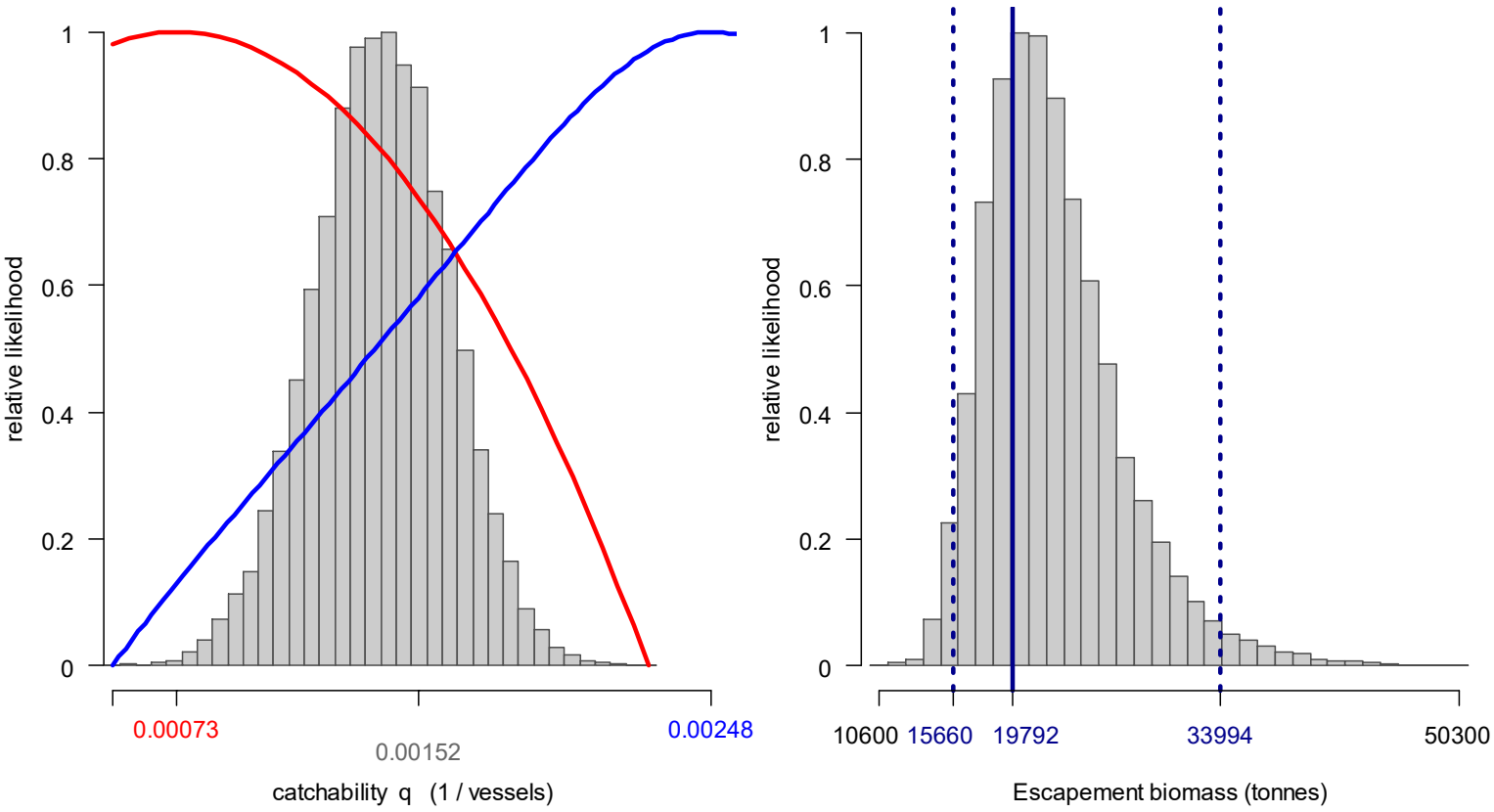

Figure 7. South sub-area. Left: Likelihood distributions for *D. gahi* catchability. Red line: prior model (pre-season survey data), blue line: in-season depletion model, grey bars: combined Bayesian model posterior. Right: Likelihood distribution (grey bars) of escapement biomass, from Bayesian posterior and average individual squid weight at the end of the season. Blue lines: maximum likelihood and 95% confidence interval. Note correspondence to Figure 8.

The MCMC distribution of the Bayesian posterior multiplied by the GAM fit of average individual squid weight (Figure A1-south) gave the likelihood distribution of *D. gahi* biomass on day 276 (October 3rd) shown in Figure 7-right, with maximum likelihood and 95% confidence interval of:

$$B_{S\ day\ 276} = 19{,}792\ t \sim 95\%\ CI\ [15{,}660 – 33{,}994]\ t \quad \textbf{(8-S)}$$

On the first day of the season estimated *D. gahi* biomass south was 34,237 t ~ 95% CI [26,751 – 54,075] t (Figure 8); higher but not statistically significant ($p > 0.16$; number of overlaps of the respective re-sampling algorithms) compared to the pre-season estimate of 25,502 t [20,128

– 42,880] (Winter et al. 2021). The highest biomass estimate of the season occurred with the second immigration on day 216, reaching 37,028 t [32,798 – 52,306]. Biomass then decreased significantly; by the rule that a straight line could not be drawn through the plot (Figure 8) without intersecting the 95% confidence interval (Swartzman et al. 1992), until regaining its final peak of the season on day 256 at 31,763 t [27,222 – 47,370].

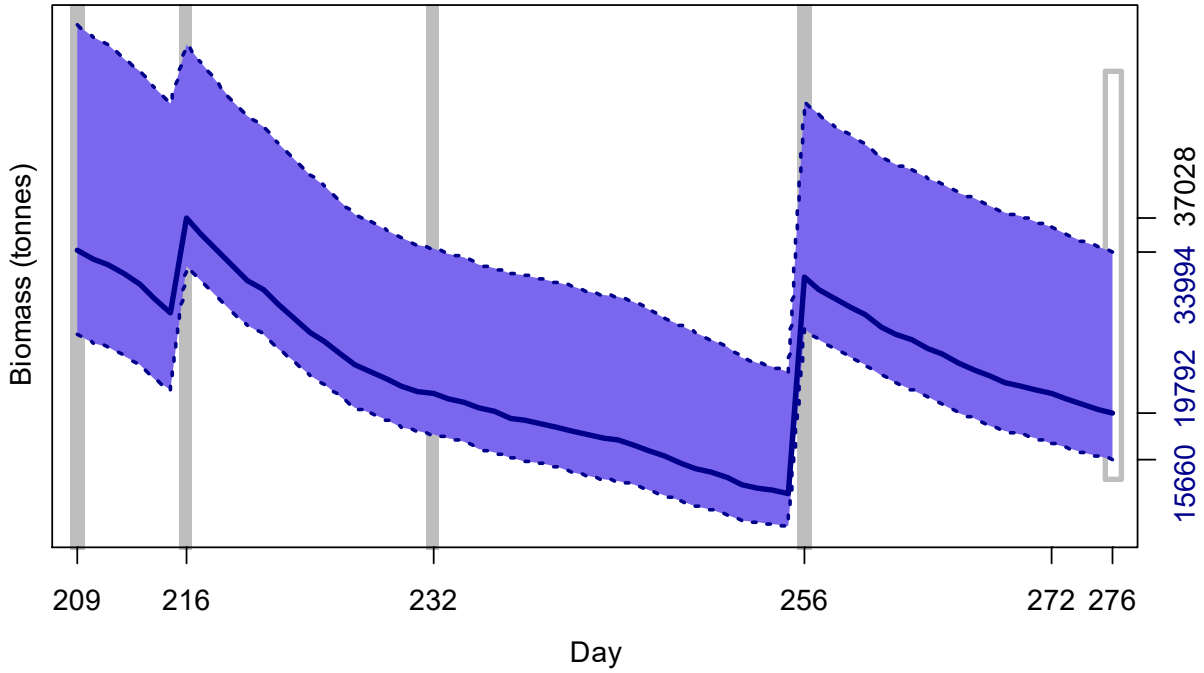

Figure 8. South sub-area. *D. gahi* biomass time series estimated from Bayesian posterior of the depletion model ± 95% confidence interval. Grey bars indicate the start of in-season depletions south; days 209, 216, 232 and 256. Note that the biomass 'footprint' on day 276 (October 3rd) corresponds to the right-side plot of Figure 7.

North

In the north sub-area, the maximum likelihood posterior ($_{Bayesian}\ q_N = 0.780 \times 10^{-3}$; Figure 9-left, and Equation **A9-N**) was preponderantly modelled on the prior ($_{prior}\ q = 0.734 \times 10^{-3}$; Figure 9-left, and Equation **A4**). The in-season depletion ($_{depletion}\ q_N = 4.823 \times 10^{-3}$; off the scale on Figure 9-left, and Equation **A6-N**) had higher weight (lower CV) than the prior in the Bayesian model (Equations **A5** and **A8-N**), but with sparse catches and effort throughout the in-season depletion did not hold a strong effect on the final combined model.

The MCMC distribution plus average individual weight variation gave the likelihood distribution of *D. gahi* biomass on day 276 (October 3rd) shown in Figure 9-right, with maximum likelihood and 95% confidence interval of:

$$B_{N\ day\ 276} = 18{,}914\ t \sim 95\%\ CI\ [13{,}962 – 37{,}568]\ t \quad \textbf{(8-N)}$$

Figure 9 [below]. North sub-area. Left: Likelihood distributions for *D. gahi* catchability. Red line: prior model (pre-season survey data), blue line: in-season depletion model, grey bars: combined Bayesian model posterior. Right: Likelihood distribution (grey bars) of escapement biomass, from Bayesian posterior and average individual squid weight at the end of the season. Green lines: maximum likelihood and 95% confidence interval. Note the correspondence to Figure 10.

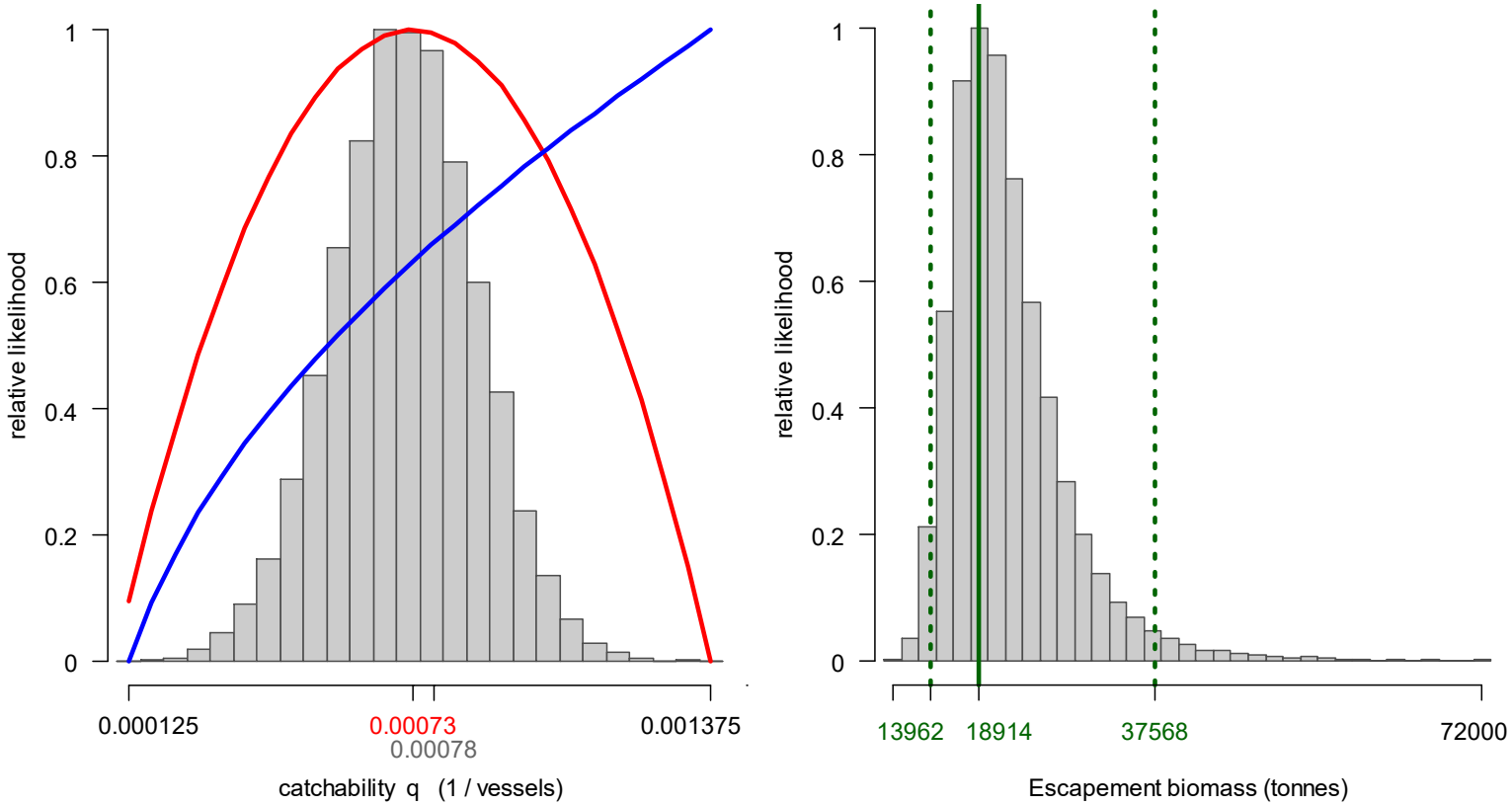

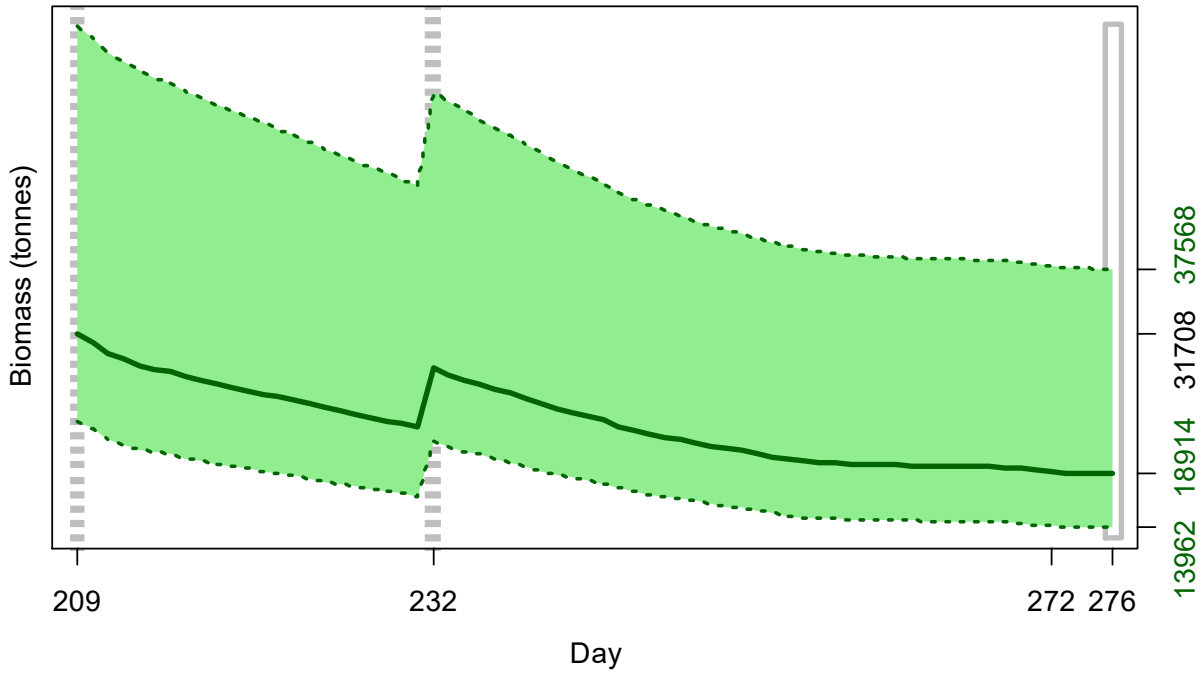

Figure 10. North sub-area. *D. gahi* biomass time series estimated from Bayesian posterior of the depletion model ± 95% confidence interval. Broken grey bars indicate the start of in-season depletions north; days 209 and 232. Note that the biomass 'footprint' on day 276 (October 3rd) corresponds to the right-side plot of Figure 9.

On the first day of the season estimated *D. gahi* biomass north was 31,708 t ~ 95% CI [23,695 – 59,769] t, which also represented the highest biomass of the season (Figure 10). This in-season biomass estimate was lower than the pre-season estimate of 52,024 t [22,430 – 116,078] (Winter et al. 2021), but owing to the high variability of both estimates was not statistically different ($p > 0.18$; number of overlaps of the respective re-sampling algorithms). Effectively, the variation of biomass estimate throughout the season was also not statistically significant (Figure 10).

Immigration

Doryteuthis gahi immigration during the season was inferred on each day by how many more squid were estimated present than the day before, minus the number caught and the number expected to have died naturally:

$$_{\text{Immigration}}N_{\text{day i}} = N_{\text{day i}} - (N_{\text{day i-1}} - C_{\text{day i-1}} - M_{\text{day i-1}})$$

where $N_{\text{day i-1}}$ are optimized in the depletion models, $C_{\text{day i-1}}$ calculated as in Equation **3**, and $M_{\text{day i-1}}$ is:

$$M_{\text{day i-1}} = (N_{\text{day i-1}} - C_{\text{day i-1}}) \times (1 - e^{-M})$$

Immigration biomass per day was then calculated as the immigration number per day multiplied by predicted average individual weight from the GAM:

$$_{\text{Immigration}}B_{\text{day i}} = {}_{\text{Immigration}}N_{\text{day i}} \times {}_{\text{GAM}}Wt_{\text{day i}}$$

All numbers N are themselves derived from the daily average individual weights, therefore the estimation automatically factors in that those squid immigrating on a given day would likely be smaller than average (because younger). Confidence intervals of the immigration estimates were calculated by applying the above algorithms to the MCMC iterations of the depletion models. Resulting total biomasses of *D. gahi* immigration north and south, up to season end (day 276), were:

$$_{\text{Immigration}}B_{\text{S season}} = 26{,}283 \text{ t} \sim 95\% \text{ CI } [18{,}695 \text{ to } 35{,}617] \text{ t} \quad \textbf{(9-S)}$$

$$_{\text{Immigration}}B_{\text{N season}} = 5{,}252 \text{ t} \sim 95\% \text{ CI } [336 \text{ to } 13{,}993] \text{ t} \quad \textbf{(9-N)}$$

Total immigration with semi-randomized addition of the confidence intervals was:

$$_{\text{Immigration}}B_{\text{Total season}} = 31{,}535 \text{ t} \sim 95\% \text{ CI } [21{,}781 \text{ to } 45{,}516] \text{ t} \quad \textbf{(9-T)}$$

In the south sub-area, the in-season peaks on days 216, 232, and 256 accounted for approximately 29.4%, 0.3%, and 62.9% of in-season immigration (start day 209 was de facto not an in-season immigration); indicative that the day 232 peak, despite clear time-series markers (Figures 5 and 6), had little influence on the overall trend (Figure 8). In the north sub-area, the in-season peak on day 232 accounted for approximately 91.0% of in-season immigration. Both south and north, the remaining immigration percentages were accounted for by the minor fluctuations throughout the season, visible on Figure 10.

Escapement biomass

Total escapement biomass was defined as the aggregate biomass of *D. gahi* at the end of day 276 (October 3rd) for south and north sub-areas combined (Equations **9-S** and **9-N**). Depletion models are calculated on the inference that all fishing and natural mortality are gathered at mid-day, thus a half day of mortality ($e^{-M/2}$) was added to correspond to the closure of the fishery at 23:59 (mid-night) on October 3rd for the final remaining vessels: Equation **10**.

$$B_{\text{Total day 276}} = (B_{\text{S day 276}} + B_{\text{N day 276}}) \times e^{-M/2}$$

$$= 38{,}706 \text{ t} \times 0.99336$$

$$= 38{,}449 \text{ t} \sim 95\% \text{ CI } [31{,}946 – 64{,}309] \text{ t} \quad \textbf{(10)}$$

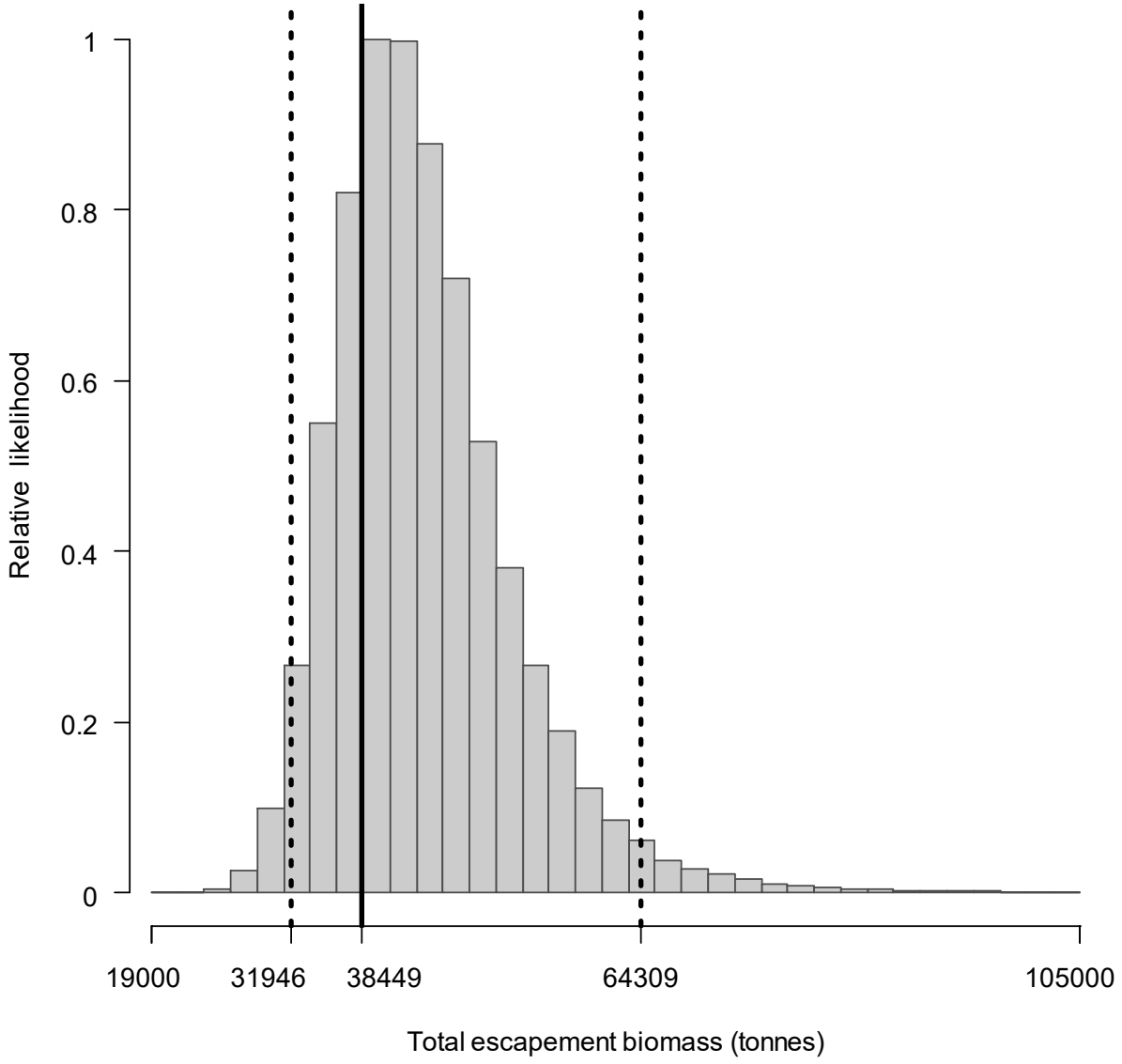

Figure 11. Likelihood distribution with 95% confidence interval of total *D. gahi* escapement biomass at the season end (October 3rd).

South and north biomass time series were moderately correlated at R = +0.4225). Semi-randomized addition of the south and north distributions gave the aggregate likelihood of total escapement biomass ($B_{\text{Total day 276}}$) shown in Figure 11[d]. The estimated escapement biomass of 38,449 t was the highest for any second season since at least 2004. The risk of the fishery in the current season, defined as the proportion of the total escapement biomass distribution below the conservation limit of 10,000 tonnes (Agnew et al. 2002, Barton 2002), was effectively zero. For comparison, the minimum aggregate biomass of the season was estimated on day 255 (September 12th) as 32,921 t ~ 95% CI [26,722 – 58,471] t; also with zero risk of < 10,000 tonnes.

Fishery bycatch

All of the 982 2nd season vessel-days (Table 1) reported *D. gahi* squid as their primary catch. The proportion of season total catch represented by *D. gahi* (34749774/35594493 = 0.976; Table A1) is the lowest for any season since 2nd season 2018. Highest bycatches in 2nd season 2021 were common rock cod *Patagonotothen ramsayi* with 444 tonnes from 976 vessel-days, common hake *Merluccius hubbsi* (253 t, 785 v-days), scallops probably *Zygochlamys* (54 t, 628 v-days), frogmouth *Cottoperca gobio* (29 t, 937 v-days), southern blue whiting *Micromesistius australis* (21 t, 103 v-days), skate Rajiformes (11 t, 830 v-days), dogfish *Squalus acanthias* (8 t, 688 v-days), and red cod *Salilota australis* (6 t, 195 v-days). Relative distributions by grid of these bycatches are shown in Figure 12; the complete list of all catches by species is in Table A1.

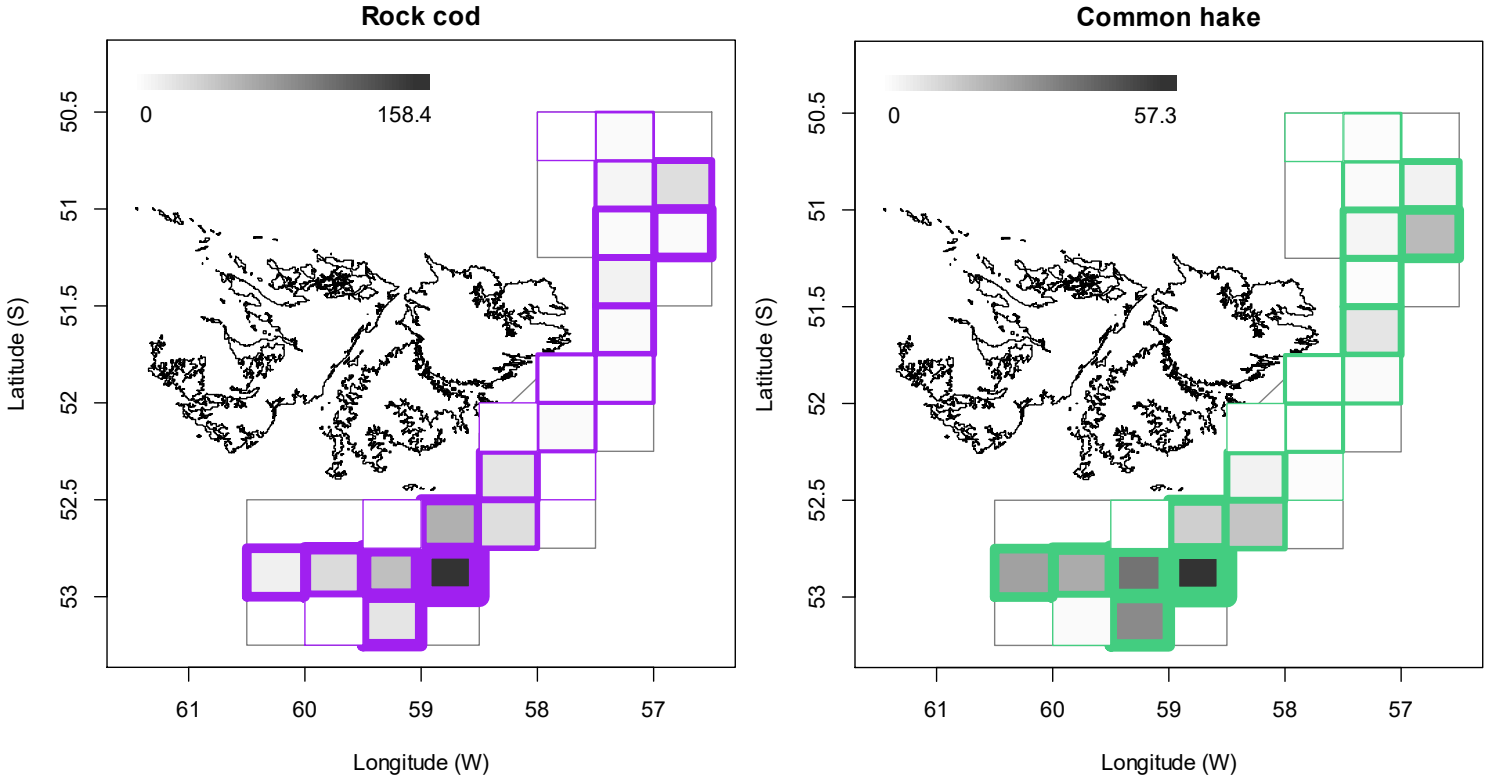

[d] Figure 11 is censored to curtail its right-skewness. The maximum distributional estimates from semi-randomized addition were >140,000 tonnes.

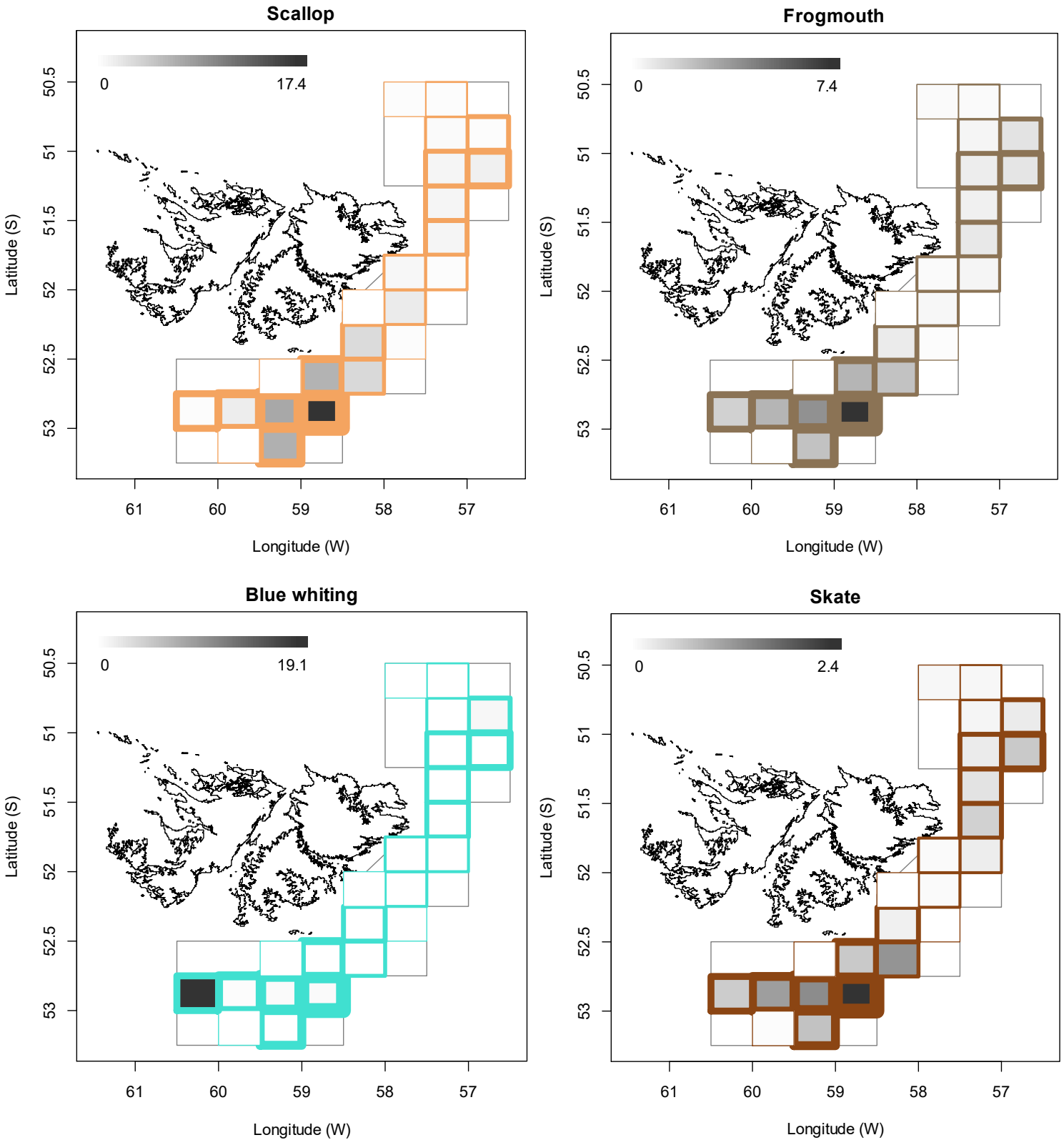

Figure 12 [above and below]. Distributions of the eight main bycatches during 2nd season 2021, by noon position grids. Thickness of grid lines is proportional to the number of vessel-days (1 to 241 per grid; 23 different grids were occupied). Grey-scale is proportional to the bycatch biomass; maximum (tonnes) indicated on each plot. For rock cod and common hake, note the contrast with Figure 4 being proportions of total reported catches per day.

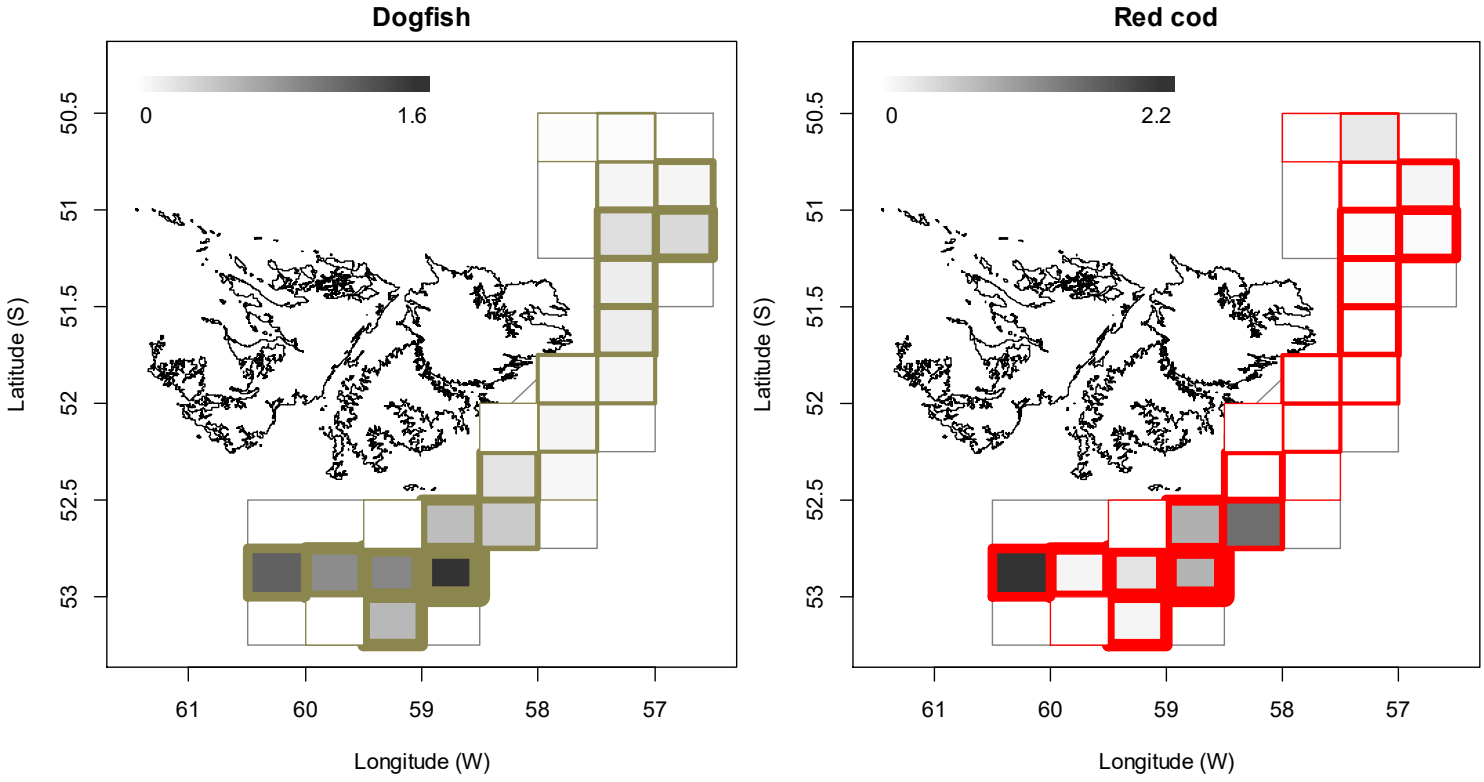

Trawl area coverage

The impact of bottom trawling on seafloor habitat has been a matter of concern in commercial fisheries (Kaiser et al. 2002; 2006), whereby the potential severity of impact relates to spatial and temporal extents of trawling (Piet and Hintzen 2012, Gerritsen et al. 2013), as well as the type of trawl gear (Rijnsdorp et al. 2020). For the *D. gahi* fishery, available catch, effort, and positional data are used to summarize the estimated 'ground' area coverage[e] occupied during the season of trawling.

The procedure for summarizing trawl area coverage is described in the Appendix of the second season 2019 report (Winter 2019). In 2nd season 2021 50% of total *D. gahi* catch was taken from 2.2% of the total area of the Loligo Box, corresponding approximately[f] to the aggregate of grounds trawled ≥9.7 times. 90% of total *D. gahi* catch was taken from 11.4% of the total area of the Loligo Box, corresponding approximately to the aggregate of grounds trawled ≥2.6 times. 100% of total *D. gahi* catch over the season was taken from 18.4% of the total area of the Loligo Box, obviously corresponding to the aggregate of all grounds trawled at least once (Figure 13 - left). The 18.4% total trawl area coverage is the highest among the seven seasons that have been given this analysis so far; narrowly higher than 2nd season last year (Winter 2020): 17.6%. Averaged by 5 × 5 km grid (Figure 13 - right), 19 grids (out of 1383) had coverage of 10 or more (that is to say, every patch of ground within that 5 × 5 km

[e] Appropriate spatial scale for calculating area coverage is a matter of some debate (Amoroso et al. 2018, Kroodsma et al. 2018). Given the comparatively small area of the Loligo Box, a high resolution of 5 km × 5 km was used for these calculations.

[f] However, not exactly. There is an expected strong correlation between the density of *D. gahi* catch taken from area units and how often these area units were trawled, but the correlation is not perfectly monotonic.

was on average trawled over 10 times or more). Forty-nine grids had coverage of 5 or more, and 132 grids had coverage of 2 or more.

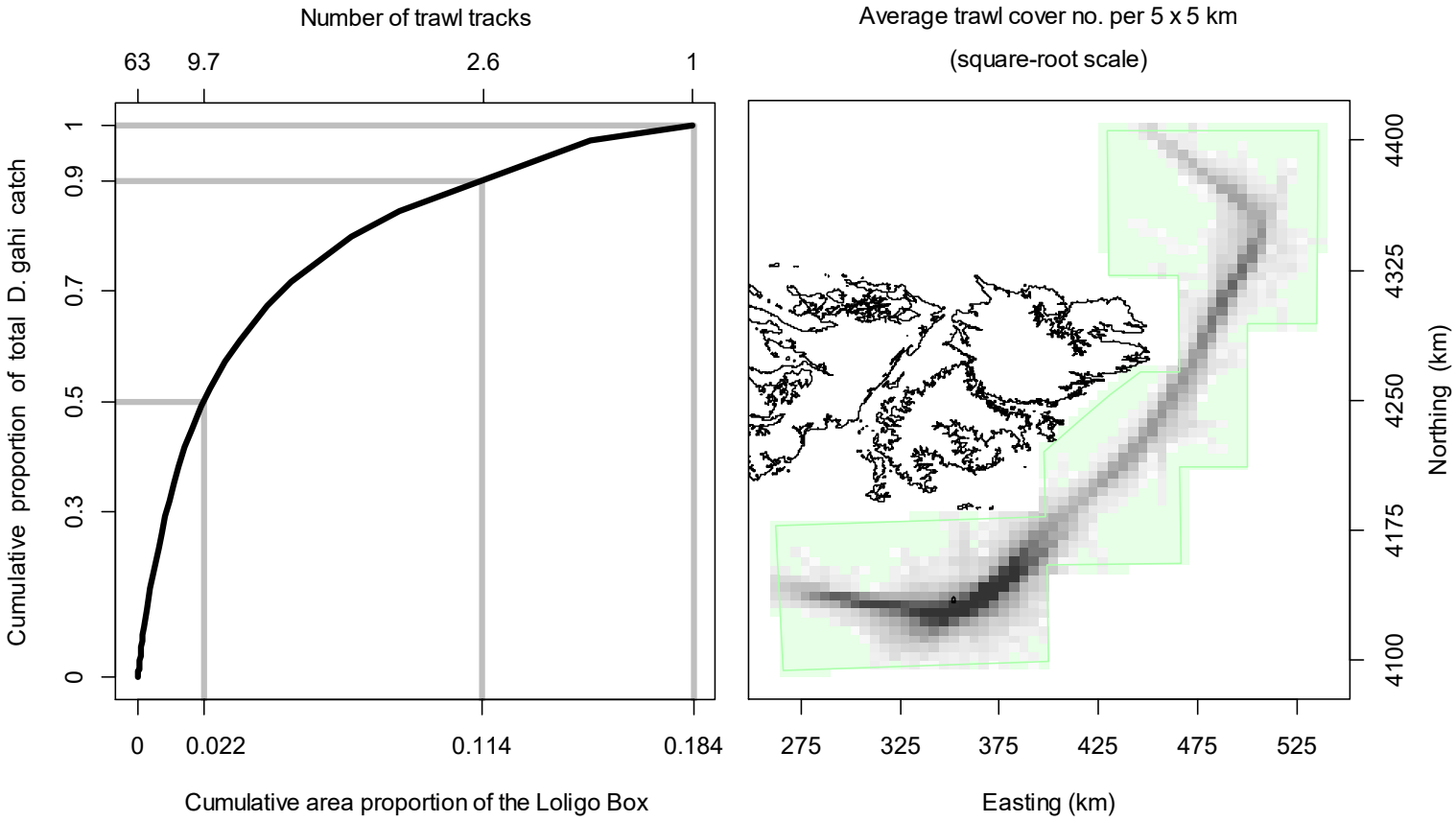

Figure 13. Left: cumulative *D. gahi* catch of 2nd season 2021, vs. cumulative area proportion of the Loligo Box the catch was taken from. The maximum number of times that any single area unit was trawled was 63, and catch cumulation by reverse density corresponded approximately to the trawl multiples shown on the top x-axis. Right: trawl cover averaged by 5 × 5 km grid; green area represents zero trawling.

Catch verification

Between September 15th and 23rd, partial catch verifications were conducted by FIFD Operations staff on four X-licensed vessels during the course of their off-loads (T. Costelloe, FIFD, pers. comm.). For each catch verification 200 boxes of *D. gahi* product were selected opportunistically and weighed on an electronic scale that was re-checked at intervals against calibration weights. Each vessel's 200 verified box weights were compared with its declared average box weight using a one-sample t-test, and the ratio difference was calculated between verified and declared average box weights. Results are summarized in Table 3. Absolute values of average verified and declared weights are not shown to minimize identifiability of individual vessels.

Two of the four vessels had significantly ($p < 0.05$) lower average verified weights than declared weight, and one vessel had significantly higher average verified weight than declared weight. Significances of weight ratios did not show any correlation with coefficients of

variation (standard deviation divided by mean) among sets of verified weights. With only four vessels, calculation of a standardized total ratio of deviation was not undertaken, but the simple average weight ratio would be –0.116%; equivalent to the total season catch being 34,709.5 tonnes rather than 34,750 tonnes.

Table 3. Ratios of average verified vs. declared average weights of four X-licence catch verifications. N: numbers of boxes of *D. gahi* product weighed for verification.

Vessel	N	wt. ratio verified / declared	p (t-test)
1	200	–0.49%	< 0.001
2	200	+0.10%	> 0.500
3	200	+3.17%	< 0.001
4	200	–3.24%	< 0.001

References

Agnew, D.J., Baranowski, R., Beddington, J.R., des Clers, S., Nolan, C.P. 1998. Approaches to assessing stocks of *Loligo gahi* around the Falkland Islands. Fisheries Research 35: 155-169.

Agnew, D. J., Beddington, J. R., and Hill, S. 2002. The potential use of environmental information to manage squid stocks. Canadian Journal of Fisheries and Aquatic Sciences, 59: 1851–1857.

Akaike, H. 1973. Information theory and an extension of the maximum likelihood principle. 2nd International Symposium on Information Theory: 267-281.

Amoroso, R.O., Parma, A.M., Pitcher, C.R., McConnaughey, R.A., Jennings, S. 2018. Comment on "Tracking the global footprint of fisheries". Science 361: eaat6713.

Arkhipkin, A. 1993. Statolith microstructure and maximum age of *Loligo gahi* (Myopsida: Loliginidae) on the Patagonian Shelf. Journal of the Marine Biological Association of the UK 73: 979-982.

Arkhipkin, A.I., Middleton, D.A.J. 2002. Sexual segregation in ontogenetic migrations by the squid *Loligo gahi* around the Falkland Islands. Bulletin of Marine Science 71: 109-127.

Arkhipkin, A.I., Middleton, D.A.J., Barton, J. 2008. Management and conservation of a short-lived fishery resource: *Loligo gahi* around the Falkland Islands. American Fisheries Society Symposium 49: 1243-1252.

Arkhipkin, A.I., Hendrickson, L.C., Payá, I., Pierce, G.J., Roa-Ureta, R.H., Robin, J.-P., Winter, A. 2021. Stock assessment and management of cephalopods: advances and challenges for short-lived fishery resources. ICES Journal of Marine Science 78: 714-730.

Barton, J. 2002. Fisheries and fisheries management in Falkland Islands Conservation Zones. Aquatic Conservation: Marine and Freshwater Ecosystems 12: 127–135.

Brooks, S.P., Gelman, A. 1998. General methods for monitoring convergence of iterative simulations. Journal of computational and graphical statistics 7:434-455.

Carlson, J.E. 2014. A generalization of Pythagoras's theorem and application to explanations of variance contributions in linear models. Research Report No. RR-14-18, Princeton, NJ: Educational Testing Service. 17 p.

Claes, J. 2021. Observer Report 1303. Technical Document, FIG Fisheries Department. 23 p.

DeLury, D.B. 1947. On the estimation of biological populations. Biometrics 3: 145-167.

Evans, D. 2021. Observer Report 1302. Technical Document, FIG Fisheries Department. 23 p.

FIFD. 2004. Fishery Report, *Loligo gahi*, Second Season 2004. Fishing statistics, biological trends, and stock assessment. Technical Document, Falkland Islands Fisheries Department. 15 p.

Gamerman, D., Lopes, H.F. 2006. Markov Chain Monte Carlo. Stochastic simulation for Bayesian inference. 2nd edition. Chapman & Hall/CRC.

Gerritsen, H.D., Minto, C., Lordan, C. 2013. How much of the seabed is impacted by mobile fishing gear? Absolute estimates from Vessel Monitoring System (VMS) point data. ICES Journal of Marine Science 70: 523-531.

Goyot, L., Derbyshire, C., Jones, J., Tutjavi, V., Winter, A. 2019. *Doryteuthis gahi* stock assessment survey, 2nd season 2019. Technical Document, Falkland Islands Fisheries Department. 20 p.

Hoenig, J.M. 1983. Empirical use of longevity data to estimate mortality rates. Fishery Bulletin 82: 898-903

Kaiser, M.J., Collie, J.S., Hall, S.J., Jennings, S., Poiner, I.R. 2002. Modification of marine habitats by trawling activities: prognosis and solutions. Fish and Fisheries 3: 114-136.

Kaiser, M.J., Clarke, K.R., Hinz, H., Austen, M.C.V., Somerfield, P.J., Karakassis, I. 2006. Global analysis of response and recovery of benthic biota to fishing. Marine Ecology Progress Series 311: 1-14.

Kroodsma, D.A., Mayorga, J., Hochberg, T., Miller, N.A., Boerder, K., Ferretti, F., Wilson, A., Bergman, B., White, T.D., Block, B.A., Woods, P., Sullivan, B., Costello, C., Worm, B. 2018. Response to Comment on "Tracking the global footprint of fisheries". Science 361: eaat7789.

Lipiński, M. R. 1979. Universal maturity scale for the commercially important squids (Cephalopoda: Teuthoidea). The results of maturity classification of *Illex illecebrosus* (Le Sueur 1821) population for years 1973–1977. ICNAF Research Document 79/11/38, 40 p.

Magnusson, A., Punt, A., Hilborn, R. 2013. Measuring uncertainty in fisheries stock assessment: the delta method, bootstrap, and MCMC. Fish and Fisheries 14: 325-342.

Matošević, N. 2021. Observer Report 1305. Technical Document, FIG Fisheries Department. 27 p.

Nash, J.C., Varadhan, R. 2011. optimx: A replacement and extension of the optim() function. R package version 2011-2.27. http://CRAN.R-project.org/package=optimx

Patterson, K.R. 1988. Life history of Patagonian squid *Loligo gahi* and growth parameter estimates using least-squares fits to linear and von Bertalanffy models. Marine Ecology Progress Series 47: 65-74.

Payá, I. 2006. Fishery Report. *Loligo gahi*, Second Season 2006. Fishery statistics, biological trends, stock assessment and risk analysis. Technical Document, Falkland Islands Fisheries Dept. 40 p.

Payá, I. 2010. Fishery Report. *Loligo gahi*, Second Season 2009. Fishery statistics, biological trends, stock assessment and risk analysis. Technical Document, Falkland Islands Fisheries Dept. 54 p.

Pierce, G.J., Guerra, A. 1994. Stock assessment methods used for cephalopod fisheries. Fisheries Research 21: 255–285.

Piet, G.J., Hintzen, N.T. 2012. Indicators of fishing pressure and seafloor integrity. ICES Journal of Marine Science 69: 1850-1858.

Plet-Hansen, K.S., Larsen, E., Mortensen, L.O., Nielsen, J.R., Ulrich, C. 2018. Unravelling the scientific potential of high resolution fishery data. Aquatic Living Resources 31:24.

Punt, A.E., Hilborn, R. 1997. Fisheries stock assessment and decision analysis: the Bayesian approach. Reviews in Fish Biology and Fisheries 7:35-63.

Rijnsdorp, A.D., Hiddink, J.G., van Denderen, P.D., Hintzen, N.T., Eigaard, O.R., Valanko, S., Bastardie, F., Bolam, S.G., Boulcott, P., Egekvist, J., Garcia, C., van Hoey, G., Jonsson, P., Laffargue, P., Nielsen, J.R., Piet, G.J., Sköld, M., van Kooten, T. 2020. Different bottom trawl fisheries have a differential impact on the status of the North Sea seafloor habitats. ICES Journal of Marine Science 77: 1772–1786.

Roa-Ureta, R. 2012. Modelling in-season pulses of recruitment and hyperstability-hyperdepletion in the *Loligo gahi* fishery around the Falkland Islands with generalized depletion models. ICES Journal of Marine Science 69: 1403–1415.

Roa-Ureta, R., Arkhipkin, A.I. 2007. Short-term stock assessment of *Loligo gahi* at the Falkland Islands: sequential use of stochastic biomass projection and stock depletion models. ICES Journal of Marine Science 64: 3-17.

Rosenberg, A.A., Kirkwood, G.P., Crombie, J.A., Beddington, J.R. 1990. The assessment of stocks of annual squid species. Fisheries Research 8: 335-350.

Santana, N. In preparation. Observer Report 1309. Technical Document, FIG Fisheries Department.

Shaw, P.W., Arkhipkin, A.I., Adcock, G.J., Burnett, W.J., Carvalho, G.R., Scherbich, J.N., Villegas, P.A. 2004. DNA markers indicate that distinct spawning cohorts and aggregations of Patagonian squid, *Loligo gahi*, do not represent genetically discrete subpopulations. Marine Biology, 144: 961-970.

Swartzman, G., Huang, C., Kaluzny, S. 1992. Spatial analysis of Bering Sea groundfish survey data using generalized additive models. Canadian Journal of Fisheries and Aquatic Sciences 49: 1366-1378.

Winter, A. 2014. *Loligo* stock assessment, second season 2014. Technical Document, Falkland Islands Fisheries Department. 30 p.

Winter, A. 2019. Stock assessment – Falkland calamari *Doryteuthis gahi* 2nd season 2019. Technical Document, Falkland Islands Fisheries Department. 36 p.

Winter, A. 2020. Stock assessment –Falkland calamari *Doryteuthis gahi* 2nd season 2020. Technical Document, Falkland Islands Fisheries Department. 32 p.

Winter, A., Arkhipkin, A. 2015. Environmental impacts on recruitment migrations of Patagonian longfin squid (*Doryteuthis gahi*) in the Falkland Islands with reference to stock assessment. Fisheries Research 172: 85-95.

Winter, A., Ramos, J.E., Shcherbich, Z., Tutjavi, V., Matošević, N. 2020. Falkland calamari (*Doryteuthis gahi*) stock assessment survey, 2nd season 2020. Technical Document, Falkland Islands Fisheries Department. 17 p.

Winter, A., Trevizan, T., Shcherbich, Z., Claes, J. 2021. Falkland calamari (*Doryteuthis gahi*) 2nd pre-season 2021 stock assessment survey. Technical Document, Falkland Islands Fisheries Department. 16 p.

Appendix
***Doryteuthis gahi* individual weights**

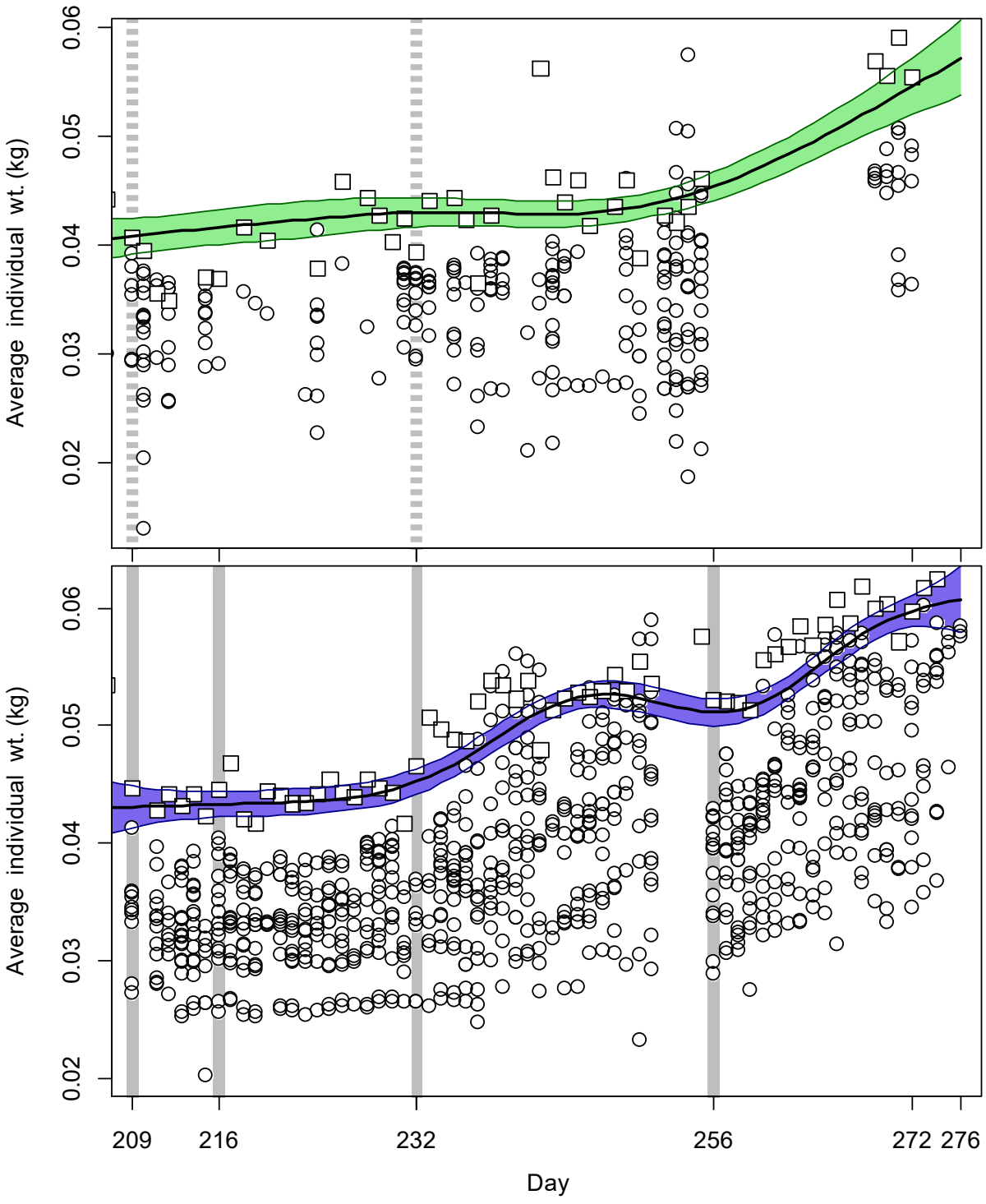

Figure A1. North (top) and south (bottom) sub-area daily average individual *D. gahi* weights from commercial size categories per vessel (circles) and observer measurements (squares). GAMs of the daily trends ± 95% confidence interval (centre lines and colour under-shading).

To smooth fluctuations, GAM trends were calculated of daily average individual weights. North and south sub-areas were calculated separately. For continuity, GAMs were calculated

using all pre-season survey and in-season data contiguously. North and south GAMs were first calculated separately on the commercial and observer data. Commercial data GAMs were taken as the baseline trends, and calibrated to observer data GAMs in proportion to the correlation between commercial data and observer data GAMs. For example, if the season average individual weight estimate from commercial data was 0.052 kg, the season average individual weight estimate from observer data was 0.060 kg, and the coefficient of determination (R^2) between commercial and observer GAM trends was 86%, then the resulting trend of daily average individual weights was calculated as the commercial data GAM values + (0.060 – 0.052) × 0.86. This way, both the greater day-to-day consistency of the commercial data trends, and the greater point value accuracy of the observer data are represented in the calculations. GAM plots of the north and south sub-areas are in Figure A1.

Prior estimates and CV

The pre-season survey had estimated *D. gahi* biomass of 77,526 tonnes (Winter et al. 2021). Hierarchical bootstrapping of the inverse distance weighting algorithm obtained a coefficient of variation (CV) equal to 28.4% of the survey biomass distribution. From modelled survey catchability, Payá (2010) had estimated average net escapement of up to 22%, which was added to the CV:

$$77{,}526 \pm (.284 + .22) = 77{,}526 \pm 50.4\% = 77{,}526 \pm 39{,}091 \text{ t} \quad \textbf{(A1)}$$

The 22% escapement was added as a linear increase in the variability, but was not used to reduce the total estimate, because squid that escape one trawl are likely to be part of the biomass concentration that is available to the next trawl.

D. gahi numbers from the survey were estimated as the survey biomasses divided by the GAM-predicted individual weight average for the survey: 0.0420 kg. The average coefficient of variation (CV) of the GAM over the duration of the pre-season survey was 3.3%, and CV of the length-weight conversion relationship (Equation **7**) was 6.6%. Joining these sources of variation with the pre-season survey biomass estimates and individual weight averages (above) gave estimated *D. gahi* numbers at survey end (day 207) of:

$$\begin{aligned} {}_{\text{prior}}\text{N}_{\text{day 207}} &= \frac{77{,}526 \times 1000}{0.0420} \pm \sqrt{50.4\%^2 + 3.3\%^2 + 6.6\%^2} \\ &= 1.845 \times 10^9 \pm 51.0\% \end{aligned} \quad \textbf{(A2)}$$

The combined catchability coefficient (q) prior was taken on day 209, the first day of the season, when 10 vessels fished in the south sub-area and 6 vessels fished in the north sub-area (Figure 3). Abundance on day 209 was discounted for natural mortality over the 2 days since the end of the survey:

$${}_{\text{prior}}\text{N}_{\text{day 209}} = {}_{\text{prior}}\text{N}_{\text{day 207}} \times e^{-M\cdot(209-207)} - \text{CNMD}_{\text{day 209}} = 1.797 \times 10^9 \quad \textbf{(A3)}$$

where $\text{CNMD}_{\text{day 209}} = 0$ as no catches intervened between the end of the survey and the start of commercial season. Thus:

$$\begin{aligned} {}_{\text{prior}}q &= \text{C(N)}_{\text{day 209}} / ({}_{\text{prior}}\text{N}_{\text{day 209}} \times \text{E}_{\text{day 209}}) \\ &= (\text{C(B)}_{\text{day 209}} / \text{Wt}_{\text{day 209}}) / ({}_{\text{prior}}\text{N}_{\text{day 209}} \times \text{E}_{\text{day 209}}) \end{aligned}$$

$$= (899.7\text{ t} / 0.0426\text{ kg}) / (1.797 \times 10^{9} \times 16\text{ vessel-days})$$

$$= 0.734 \times 10^{-3}\ \text{vessels}^{-1}\ ^{g} \qquad \textbf{(A4)}$$

$SD_{\text{prior q}}$ (Equation **4**) was calculated as $_{\text{prior}}q$ multiplied by its CV. $CV_{\text{prior q}}$ was calculated as the sum of variability in $_{\text{prior}}N_{\text{day 209}}$ (Equation **A2**) plus variability in the catches of vessels on start day 209, plus variability of the natural mortality (see Appendix section Natural mortality).

$$CV_{\text{prior q}} = \sqrt{51.0\%^2 + \left(\frac{SD\,(C(B)_{\text{vessels day 209}})}{\text{mean}\,(C(B)_{\text{vessels day 209}})}\right)^2 + (1-(1-CV_M)^{(209\text{ - mid\_survey})})^2}$$

$$= \sqrt{51.0\%^2 + 57.8\%^2 + 78.1\%^2} = 109.7\%$$

$$SD_{\text{prior q}} = {}_{\text{prior}}q \times CV_{\text{prior q}} = 0.806 \times 10^{-3}\ \text{vessels}^{-1} \qquad \textbf{(A5)}$$

Depletion model estimates and CV

For the south sub-area, the equivalent of Equation **2** with four N_{day} was optimized on the difference between predicted and actual catches (Equation **3**), resulting in parameters values:

$$_{\text{depletion}}N1_{\text{S day 209}} = 0.499 \times 10^{9}; \quad _{\text{depletion}}N2_{\text{S day 216}} = 0.268 \times 10^{6}$$

$$_{\text{depletion}}N3_{\text{S day 232}} = 0.159 \times 10^{-6}; \quad _{\text{depletion}}N4_{\text{S day 256}} = 0.315 \times 10^{6}$$

$$_{\text{depletion}}q_{\text{S}} = 2.479 \times 10^{-3}\ ^{h} \qquad \textbf{(A6-S)}$$

The normalized root-mean-square deviation of predicted vs. actual catches was calculated as the CV of the model:

$$CV_{\text{rmsd S}} = \frac{\sqrt{\sum_{i=1}^{n}\left({}_{\text{predicted}}C(N)_{\text{S day i}} - {}_{\text{actual}}C(N)_{\text{S day i}}\right)^2 / n}}{\text{mean}\left({}_{\text{actual}}C(N)_{\text{S day i}}\right)}$$

$$= 2.439 \times 10^{6} / 9.199 \times 10^{6} = 26.5\% \qquad \textbf{(A7-S)}$$

$CV_{\text{rmsd S}}$ was added to the variability of the GAM-predicted individual weight averages for the season (Figure A1-S); equal to a CV of 1.25% south. CVs of the depletion were then calculated as the sum:

$$CV_{\text{depletion S}} = \sqrt{CV_{\text{rmsd S}}^{\ 2} + CV_{\text{GAM Wt S}}^{\ 2}} = \sqrt{26.5\%^2 + 1.25\%^2}$$

$$= 26.5\% \qquad \textbf{(A8-S)}$$

For the north sub-area, the Equation **2** equivalent with two N_{day} was optimized on the difference between predicted and actual catches (Equation **3**), resulting in parameter values:

[g] On Figure 7-left and Figure 9-left.
[h] On Figure 7-left.

$$_{\text{depletion}}N1_{\text{N day 209}} = 0.156 \times 10^{9}; \qquad _{\text{depletion}}N2_{\text{N day 232}} = 0.068 \times 10^{9}$$

$$_{\text{depletion}}q_{\text{N}} = 4.823 \times 10^{-3}\ ^{i} \qquad \textbf{(A6-N)}$$

Root-mean-square deviation of predicted vs. actual catches was calculated as the CV of the model:

$$CV_{\text{rmsd N}} = \frac{\sqrt{\sum_{i=1}^{n}\left({}_{\text{predicted}}C(N)_{\text{N day i}} - {}_{\text{actual}}C(N)_{\text{N day i}}\right)^2 / n}}{\text{mean}\left({}_{\text{actual}}C(N)_{\text{N day i}}\right)}$$

$$= 1.475 \times 10^{6} / 1.647 \times 10^{6} = 89.6\% \qquad \textbf{(A7-N)}$$

$CV_{\text{rmsd N}}$ was added to the variability of the GAM-predicted individual weight averages for the season (Figure A1-N); equal to a CV of 1.77% north. CVs of the depletion were then calculated as the sum:

$$CV_{\text{depletion N}} = \sqrt{CV_{\text{rmsd N}}^{\ 2} + CV_{\text{GAM Wt N}}^{\ 2}} = \sqrt{89.6\%^2 + 1.77\%^2}$$

$$= 89.6\% \qquad \textbf{(A8-N)}$$

Combined Bayesian models

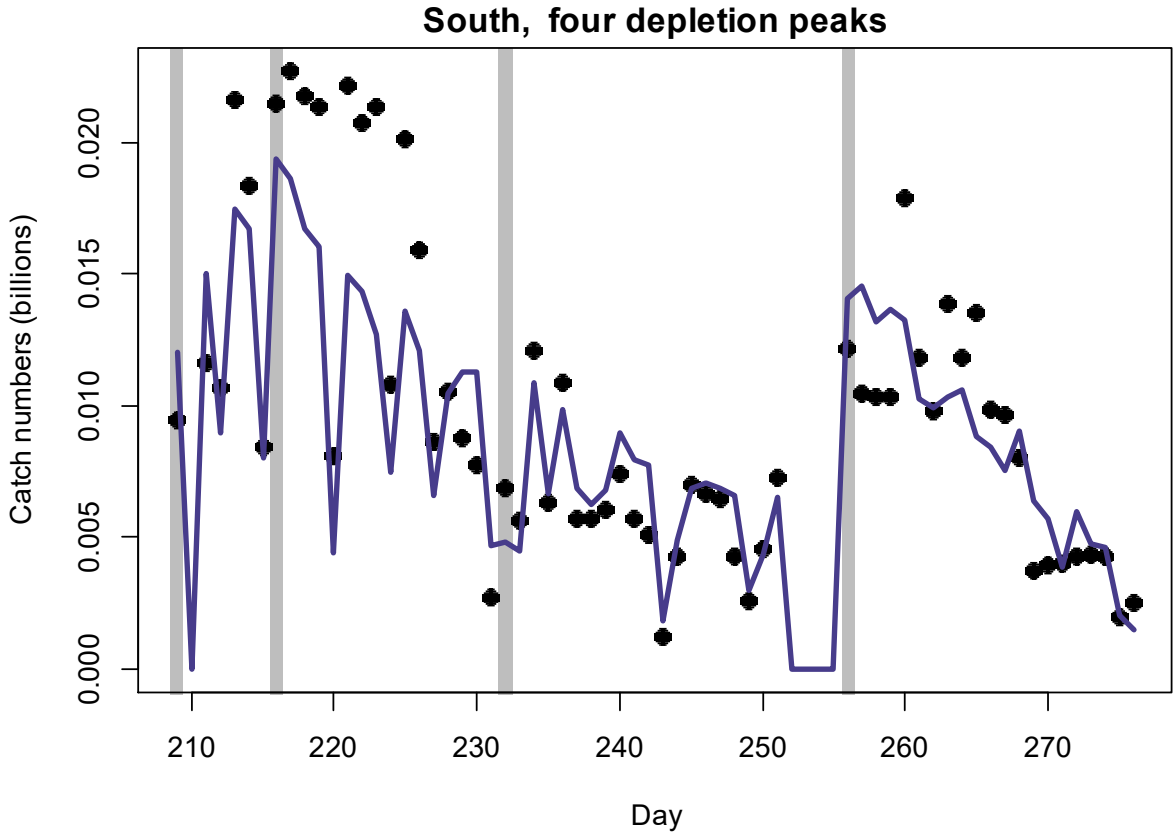

[i] Off the scale on Figure 9-left.

Figure A2-S [previous page]. Daily catch numbers estimated from actual catch (black points) and predicted from the depletion model (purple line) in the south sub-area.

For the south sub-area, joint optimization of Equations **3** and **4** resulted in parameters values:

$$\text{Bayesian } N1_{\text{S day 209}} = 0.794 \times 10^{9}; \quad \text{Bayesian } N2_{\text{S day 216}} = 0.209 \times 10^{9}$$

$$\text{Bayesian } N3_{\text{S day 232}} = 0.800 \times 10^{-6}; \quad \text{Bayesian } N4_{\text{S day 256}} = 0.376 \times 10^{9}$$

$$\text{Bayesian } q_{\text{S}} = 1.523 \times 10^{-3}\ ^{j} \qquad \textbf{(A9-S)}$$

These parameters produced the fit between predicted catches and actual catches shown in Figure A2-S.

For the north sub-area, joint optimization of Equations **3** and **4** resulted in parameters values:

$$\text{Bayesian } N1_{\text{N day 209}} = 0.776 \times 10^{9}; \quad \text{Bayesian } N2_{\text{N day 232}} = 0.137 \times 10^{9}$$

$$\text{Bayesian } q_{\text{N}} = 0.780 \times 10^{-3}\ ^{k} \qquad \textbf{(A9-N)}$$

These parameters produced the fit between predicted catches and actual catches shown in Figure A2-N.

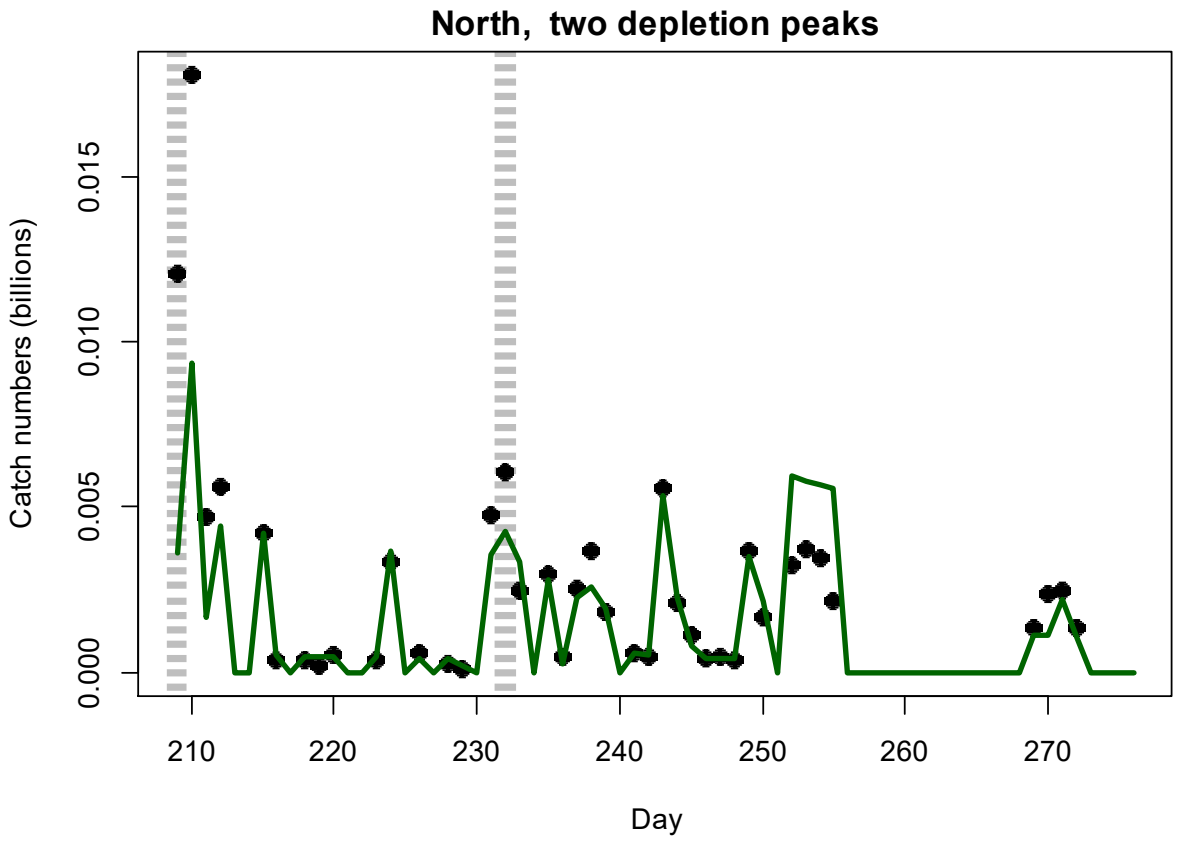

Figure A2-N. Daily catch numbers estimated from actual catch (black points) and predicted from the depletion model (green line) in the north sub-area.

[j] On Figure 7-left.
[k] On Figure 9-left.

Natural mortality

Natural mortality is parameterized as a constant instantaneous rate M = 0.0133 day^{-1} (Roa-Ureta and Arkhipkin 2007), based on Hoenig's (1983) log mortality vs. log maximum age regression, applied to an estimated maximum age of 352 days for *D. gahi*:

$$\log(M) = 1.44 - 0.982 \times \log(age_{max})$$

$$M = \exp(1.44 - 0.982 \times \log(352))$$

$$= 0.0133 \quad \textbf{(A10)}$$

Hoenig (1983) derived Equation **A10** from the regression of 134 stocks among 79 species of fish, molluscs, and cetaceans. Hoenig's regression obtained $R^2 = 0.82$, but a corresponding coefficient of variation (CV) was not published. An approximate CV of M was estimated by measuring the coordinates off a print of Figure 1 in Hoenig (1983) and repeating the regression. Variability of M was calculated by randomly re-sampling, with replacement, the regression coordinates 10000× and re-computing Equation **A10** for each iteration of the resample. The CV of M from the 10000 random resamples was:

$$CV_M = SD_M / Mean_M$$

$$CV_M = 0.0021 / 0.0134 = 15.46\% \quad \textbf{(A11)}$$

CV_M was aggregated over the number of days between the midpoint of the survey and the commercial season start, rather than between the end of the survey and commercial season start, as the midpoint more accurately reflects how much time has elapsed since the fishing area on average was surveyed. The midpoint of the survey was calculated as the mean day weighted by the number of survey trawls taken per day:

$$\text{mid\_survey} = \frac{\Sigma\left(\text{day} \times N_{\text{survey trawls}}|_{\text{day}}\right)}{\Sigma\left(N_{\text{survey trawls}}|_{\text{day}}\right)} = 199.95^{[1]} \quad \textbf{(A12)}$$

CV_M was thus further indexed by $1 - (1 - CV_M)$ to ensure that the value could not decrease if CV_M was hypothetically > 100%:

$$1 - (1 - CV_M)^{(\text{commercial season start} - \text{mid\_survey})} \quad \textbf{(A13)}$$

Equation **A13** is included in Equation **A5**.

Total catch by species

Table A1 [next page]: Total reported catches and discard by taxon during 2nd season 2021 X-license fishing, and number of catch reports in which each taxon occurred. Does not include incidental catches of pinnipeds or seabirds.

[1] In common nomenclature day 199 and day 200 are July 18th and July 19th.

Species Code	Species / Taxon	Catch Wt. (KG)	Discard Wt. (KG)	N Reports
LOL	*Doryteuthis gahi*	34749774	47613	982
PAR	*Patagonotothen ramsayi*	444431	444431	976
HAK	*Merluccius hubbsi*	253411	11927	785
SCA	Scallop	53930	53930	628
CGO	*Cottoperca gobio*	29243	29233	937
BLU	*Micromesistius australis*	21480	21116	103
RAY	Rajiformes	11071	9412	830
DGH	*Schroederichthys bivius*	7790	7790	688
BAC	*Salilota australis*	6382	1428	195
KIN	*Genypterus blacodes*	3267	858	61
PTE	*Patagonotothen tessellata*	3157	3157	150
TOO	*Dissostichus eleginoides*	2835	2834	476
MED	Medusae sp.	1912	1912	78
ING	*Moroteuthis ingens*	1218	1218	243
OCT	*Octopus* spp.	1198	1198	252
GRV	*Macrourus* spp.	710	710	74
UCH	Sea urchin	582	582	50
DGS	*Squalus acanthias*	247	247	13
MUL	*Eleginops maclovinus*	209	209	62
SPN	Porifera	208	208	13
LIM	*Lithodes murrayi*	206	206	33
MAR	*Martialia hyadesi*	176	176	5
GRF	*Coelorhynchus fasciatus*	168	168	30
LIT	*Lithodes turkayi*	147	147	16
LIS	*Lithodes santolla*	105	105	8
ILL	*Illex argentinus*	100	100	11
EEL	*Iluocoetes fimbriatus*	97	97	57
MYX	*Myxine* spp.	83	83	35
DGX	Dogfish / Catshark	60	60	2
MUN	*Munida* spp.	47	47	4
WHI	*Macruronus magellanicus*	45	43	19
NEM	*Neophyrnichthys marmoratus*	31	31	14
SAR	*Sprattus fuegensis*	30	30	2
CHE	*Champsocephalus esox*	30	30	25
LAR	*Lampris immaculatus*	28	28	2
ALF	*Allothunnus fallai*	18	18	2
RED	*Sebastes oculatus*	18	18	12
BUT	*Stromateus brasiliensis*	15	15	6
PAT	*Merluccius australis*	13	13	6
GRC	*Macrourus carinatus*	7	7	1
SEP	*Seriolella porosa*	6	6	5
BDU	*Brama dussumieri*	3	3	1
COT	*Cottunculus granulosus*	3	3	1
CAM	*Cataetyx messieri*	2	2	1
Total		35594493	641449	982